



Cite this: DOI: 10.1039/c6ob01751g

## One-pot *N*-glycosylation remodeling of IgG with non-natural sialylglycopeptides enables glycosite-specific and dual-payload antibody–drug conjugates†

Feng Tang,<sup>a,b</sup> Yang Yang,<sup>a,c</sup> Yubo Tang,<sup>a,d</sup> Shuai Tang,<sup>a</sup> Liyun Yang,<sup>a,b</sup> Bingyang Sun,<sup>a,c</sup> Bofeng Jiang,<sup>a,c</sup> Jinhua Dong,<sup>d</sup> Hong Liu,<sup>a</sup> Min Huang,<sup>a</sup> Mei-Yu Geng<sup>a</sup> and Wei Huang<sup>\*a,c</sup>

Chemoenzymatic transglycosylation catalyzed by *endo*-S mutants is a powerful tool for *in vitro* glyco-engineering of therapeutic antibodies. In this paper, we report a one-pot chemoenzymatic synthesis of glycoengineered Herceptin using an egg-yolk sialylglycopeptide (SGP) substrate. Combining this one-pot strategy with novel non-natural SGP derivatives carrying azido or alkyne tags, glycosite-specific conjugation was enabled for the development of new antibody–drug conjugates (ADCs). The site-specific ADCs and semi-site-specific dual-drug ADCs were successfully achieved and characterized with SDS-PAGE, intact antibody or ADC mass spectrometry analysis, and PNGase-F digestion analysis. Cancer cell cytotoxicity assay revealed that small-molecule drug release of these ADCs relied on the cleavable Val-Cit linker fragment embedded in the structure. These results represent a new approach for glycosite-specific and dual-drug ADC design and rapid synthesis, and also provide the structural requirement for their biologic activities.

Received 11th August 2016,  
Accepted 2nd September 2016

DOI: 10.1039/c6ob01751g

www.rsc.org/obc

### Introduction

Therapeutic IgG-type monoclonal antibodies (mAbs) have attracted continuous research attention during the past three decades. Among the FDA approved bio-drugs, over one third is mAb, applied in clinic treatments on cancer, autoimmune diseases, and infectious diseases.<sup>1–4</sup> IgG mAb consists of two heavy chains and two light chains, forming two Fab (antigen binding) domains and one Fc (crystallizable) domain. The Fc

domain is involved in recruitment of immune cells by binding to Fc receptors on the immune cell surface, and helps direct the immune response<sup>5–9</sup> including phagocytosis, immune cell activation, and cytokine stimulation towards the antigen-displayed targets. *N*-Glycosylation on Asn<sup>297</sup> of IgG Fc mediates Fc receptor interaction and regulates antibody-dependent effector functions.<sup>9–14</sup> Core-fucosylation of Fc *N*-glycans hindered the binding with an FcγIIIa receptor and the lack of core-fucose would dramatically enhance antibody-dependent cell-mediated cytotoxicity (ADCC).<sup>12,13,15</sup> Crystallization studies on the Fc–FcγIIIa complex revealed a unique carbohydrate–carbohydrate interaction between afucosylated *N*-glycans of Fc and the FcγIIIa glycans that could be blocked by the core-fucose of Fc *N*-glycans.<sup>12</sup> Galactose on the non-reducing end of Fc *N*-glycans improves the ADCC and complement-dependent cytotoxicity (CDC) activity of IgG antibodies.<sup>16,17</sup> It is reported that the terminal sialic acid moieties of Fc *N*-glycans are crucial for the anti-inflammatory activity of intravenous immunoglobulin (IVIg).<sup>14,18–20</sup> *N*-Glycosylation also affects the pharmacokinetics and immunogenicity of therapeutic mAbs.<sup>21–24</sup>

Massive data have demonstrated the significant modulation effect of *N*-glycans on IgG functions, therefore glyco-engineering technologies have been developed and applied in structural optimization on IgG glycans for better therapeutic

<sup>a</sup>CAS Key Laboratory of Receptor Research, CAS Center for Excellence in Molecular Cell Science, Shanghai Institute of Materia Medica, Chinese Academy of Sciences, 555 Zuchongzhi Road, Pudong, Shanghai, China 201203.

E-mail: huangwei@simm.ac.cn; Fax: +86-21-50807088;

Tel: +86-21-20231000 ext. 2517

<sup>b</sup>University of Chinese Academy of Sciences, No. 19A Yuquan Road, Beijing 100049, China

<sup>c</sup>Human Institute, ShanghaiTech University, 99 Haik Road, Pudong, Shanghai, 201210 China

<sup>d</sup>Key Laboratory of Structure-Based Drug Design and Discovery, Ministry of Education, Shenyang Pharmaceutical University, Shenyang, 110016, China

† Electronic supplementary information (ESI) available: Detailed structures of **10a–d**, **21a–d**, payloads, and other small molecules; schemes of PNGase-F digestion and ADC conjugation; SDS-PAGE and LC-MS of **7a–d**, **14a–e**, T-DM1, T-MMAE, and other small molecules; synthetic procedures of **10a–d**, **21a–d**, payloads, and other small molecules; NMR spectra of all intermediates. See DOI: 10.1039/c6ob01751g

efficacy. In a review on glycoengineered mAbs,<sup>21</sup> the clinic study status, glycoengineering technologies, and the functional properties of over 15 glycoengineered IgG drug candidates were well summarized. The common technology to control IgG glycosylation is to interfere with the biosynthetic pathway of *N*-glycosylation in particular expression systems,<sup>15,25–29</sup> combined with glycosyltransferase modulation such as knock-out of the fucosyltransferase FUT8 for elimination of the core-fucose<sup>28,29</sup> and up-regulation of bisecting GlcNAc transferase GnT-III,<sup>30</sup> or *in vitro* enhanced galactylation<sup>31</sup> and sialylation<sup>32</sup> to obtain the desired *N*-glycans. Recently, several research groups have reported a chemoenzymatic method for efficient glycosylation remodeling of IgG *N*-glycans with a mutated *endo-N*-acetylglucosaminidase from *Streptococcus pyogenes* (*endo-S*).<sup>16,33,34</sup> This method features with two key steps: (1) trimming of natural glycoforms, mainly containing G0F, G1F, and G2F, with wild-type *endo-S* to cleave the glycosidic bond of a GlcNAc $\beta$ 1,4GlcNAc motif and give the deglycosylated IgG with the innermost Fuc $\alpha$ 1,6GlcNAc disaccharide or further defucosylated GlcNAc monosaccharide; (2) *endo-S* mutant-catalyzed chemoenzymatic transglycosylation of a chemically synthetic *N*-glycan oxazoline as the donor substrate onto Fuc $\alpha$ 1,6GlcNAc-IgG or GlcNAc-IgG, giving a glycoengineered antibody with a well-defined *N*-glycan structure. The substrate specificity of *endo-S* covers a quite range of biantennary complex type, mannose type (5 mannose moieties or less) and hybrid type *N*-glycans, but *endo-S* restrains on its acceptor substrate specifically for the IgG Fc domain that makes it a perfect enzyme for IgG *in vitro* glycoengineering.

Antibody–drug conjugates (ADCs) covalently connect a small-molecule drug onto an antibody *via* a suitable linker fragment. Through a high targeting effect based on antibody–antigen specific recognition, the loaded drug was delivered into the antigen-displayed target cells by endocytosis.<sup>35</sup> ADCs have shown potent therapeutic efficacy in clinic studies on treatment of various tumors.<sup>35</sup> Antitumor ADCs require the antibody with specific recognition on the over-expressed tumor biomarker in high binding affinity, and a highly potent payload such as the cytotoxic agents DM1 and MMAE.<sup>36,37</sup> The linker is also very important for remaining stable in blood flow while being rapidly released after being delivered into the tumor cells.<sup>38</sup> The launched ADC drugs or ADC candidates in clinic trials mainly conjugated at the Lys or Cys amino acids of the antibodies *via* a random way. The potential problem of random conjugation is apparent on drug quality control, precise drug–antibody ratio (DAR) control, bio-activity repeatability, *etc.* Site-specific conjugation of ADCs has become the hot topic in this field.<sup>39–41</sup> The approaches *via* incorporation of free Cys or non-natural amino acids at the specific sites of an antibody sequence for payload conjugation have been reported.<sup>42–45</sup> Besides these technologies, site-specific conjugation on IgG Fc *N*-glycans provided an alternative strategy and attracted research interest. Boons G. J. established an elegant method<sup>46</sup> for glycosite-specific ADC preparation using sialyltransferase to attach an azido-tagged sialic acid moiety onto

the galactosylated IgG *N*-glycan and conjugate a cytotoxic agent (doxorubicin) on the pre-assembled azido group *via* the “click chemistry” of cycloaddition reaction. Zhou *et al.*<sup>47</sup> reported a similar strategy to attach natural sialic acid onto Fc glycan and followed with NaIO<sub>4</sub> oxidation to give an aldehyde tag on the *N*-glycan for site-specific conjugation. The chemical oxidation of an IgG antibody in this method is a very tricky step that usually causes oxidative side reaction and protein denaturing. A galactosyltransferase mutant was employed for glycosite-specific conjugation<sup>48</sup> by transferring the keto-tagged<sup>49</sup> or azido-tagged<sup>50</sup> galactose onto the degalactosylated G0F glycoform or deglycosylated Fuc $\alpha$ 1,6GlcNAc disaccharide form of IgG.<sup>51</sup> These methods demonstrated a new avenue of glycosite-specific ADC development with a precise structure and DAR.

The glycosyltransferase-catalyzed glycosite-specific conjugation with a non-natural UDP-monosaccharide substrate was always restrained on the sugar structures with a narrow substrate specificity.<sup>52</sup> To obtain structural diversity for the screening and development of an ADC drug candidate, we sought to take advantage of *endo-S* for IgG *N*-glycosylation remodeling with various non-natural glycan substrates. Wang L. X. and co-workers reported<sup>16</sup> that *endo-S* D233Q/A could construct IgG bearing biantennary complex-type *N*-glycans in a wide range including sialylated, galactosylated, fucosylated, bisecting-GlcNAc, and azido-tagged Man3GlcNAc cores. Wong C. H's recent work<sup>34</sup> has also indicated the wide substrate specificity of this enzyme on glycan structures. In the current work, we employed a sialylglycopeptide extracted from egg yolks as the precursor<sup>53,54</sup> and synthesized a series of azido- or alkyne-tagged sialylglycopeptides for IgG glycosylation remodeling. An efficient one-pot method for the assembly of chemical handles on IgG Fc *N*-glycans was achieved by a combination of three steps in one reaction cell: (1) release of the free glycans from these non-natural sialylglycopeptide derivatives with *endo-N*-acetylglucosaminidase from *Mucor hiemalis* (*endo-M*); (2) conversion of the free glycans to their oxazoline forms as the enzyme substrate; (3) transfer of the glycan oxazolines to Fuc $\alpha$ 1,6GlcNAc-IgG catalyzed by *endo-S* D233Q. Very recently, during the preparation of this manuscript, we noticed that Davis B. G. and his co-workers have reported<sup>55</sup> another series of non-natural *N*-glycans for IgG glycoengineering *via* a similar *endo-S*-catalyzed method but with different glycan derivatives that further demonstrated the power of chemoenzymatic IgG glycosylation engineering and broad glycan substrate recognition of *endo-S* on various non-natural structures. Furthermore, with the glycoengineered IgG carrying chemical handles, we performed the site-specific conjugation of small-molecule drugs *via* various linker fragments. The antitumor assay results indicated that a suitable cleavable linker structure is extremely important for the activity of glycosite-specific ADCs. We also provide a novel strategy for dual-drug ADC<sup>56,57</sup> design by connection of one kind of small-molecule drug on the glycans and another different drug on the Lys residues *via* random conjugation. The dual-drug ADC design enables employment of dual cytotoxic mechanisms such as simultaneous anti-tublin

and DNA damaging, that could be potentially useful for better efficacy or for drug-resistance cancer treatment.

## Results and discussion

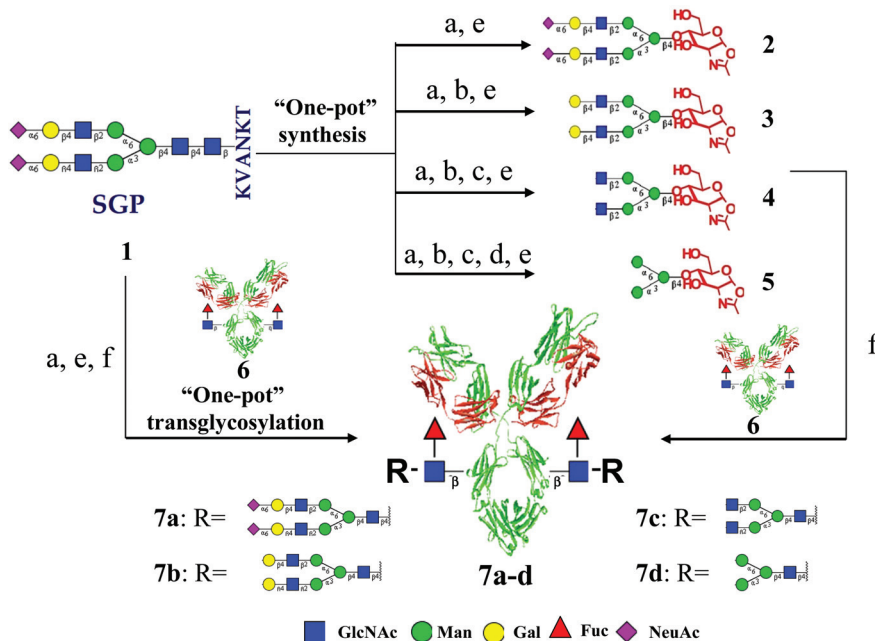
### One-pot strategy for chemoenzymatic IgG glycosylation remodeling

*endo*-Glycosidase-catalyzed chemoenzymatic synthesis was recently established for preparation of homogeneous *N*-glycopeptides, glycoproteins, and other glycoconjugates.<sup>16,58–66</sup> In this approach, *N*-glycan oxazolines were used as the glycosylation donor substrates of wild-type or mutated *endo*-glycosidases to perform transglycosylation onto a GlcNAc-containing acceptor substrate. Herein, we sought to develop a one-pot strategy for rapid synthesis of *N*-glycan oxazolines and for glycoengineering of antibody substrates. As shown in Scheme 1, we started with the one-pot semi-synthesis of various bi-antennary *N*-glycan oxazolines using the egg-yolk sialylglycopeptide (SGP, **1**)<sup>53,54</sup> as the precursor. SGP was treated with *endo*-*N*-acetylglucosaminidase from *Mucor hiemalis* (*endo*-M) to cleave the glycosidic bond of a GlcNAc $\beta$ 1,4GlcNAc motif and release the glycan, Sia<sub>2</sub>Gal<sub>2</sub>GlcNAc<sub>2</sub>Man<sub>3</sub>GlcNAc, from the hexapeptide. The *in situ* glycan was then converted to oxazoline **2** in the presence of 2-chloro-1,3-dimethylimidazolium chloride (DMC) and triethylamine following Shoda's method.<sup>67</sup> The crude oxazoline from one-pot synthesis was then subjected to solid-phase extraction (SPE) *via* a porous graphitic carbon (PGC) column and gel-filtration *via* a Sephadex G-25 column to give the purified product. Application of this one-pot semi-synthesis

was extended to prepare other bi-antennary *N*-glycan oxazolines **3–5** by combined steps of *exo*-glycosidase trimming during the procedure (Scheme 1). Neuraminidase,  $\beta$ -galactosidase, and  $\beta$ -*N*-acetylglucosaminidase (GlcNAcase) were employed to remove the non-reducing end saccharides of the released *N*-glycan from SGP in one reaction cell and followed with oxazoline formation reaction to give the respective purified Gal<sub>2</sub>GlcNAc<sub>2</sub>Man<sub>3</sub>GlcNAc oxazoline (**3**), GlcNAc<sub>2</sub>Man<sub>3</sub>GlcNAc oxazoline (**4**), and Man<sub>3</sub>GlcNAc oxazoline (**5**). High-performance anion-exchange chromatography with pulsed amperometric detection (HPAEC-PAD) monitoring on each step of enzymatic deglycosylation and oxazoline formation was performed to ensure the complete sugar truncation for homogeneous glycan oxazoline production (see the ESI†).

The rapid semi-synthesis of *N*-glycan oxazolines **2–5** by this one-pot approach provided us the donor substrate pool for chemoenzymatic glycosylation remodeling of IgG following the reported procedure.<sup>16</sup> We chose commercial mAb drug Herceptin as the model and removed its major glycoforms of G0F, G1F, and G2F by wild-type *endo*-S to give Herceptin-Fuc $\alpha$ 1,6GlcNAc (**6**) as the acceptor substrate. Chemoenzymatic transglycosylation catalyzed by *endo*-S D233Q using substrate **6** and oxazolines **2–5** offered glycoengineered Herceptin **7a–d** bearing homogeneous glycoform S2G2F (**7a**), G2F (**7b**), G0F (**7c**), and M3F (**7d**). The products were characterized with SDS-PAGE and LC-MS analysis of the intact IgG (Fig. S1–S5†). In Table 1, the deconvolution MS data of intact **7a–d** are summarized and indicate the high accordance of measured and calculated mass.

The successful one-pot semi-synthesis of *N*-glycan oxazolines encouraged us to further develop a one-pot method for



**Scheme 1** Conditions: (a) *endo*-M, phosphate buffer (PB), pH 6.5; (b) Neuraminidase, PB, pH 5.0; (c)  $\beta$ -galactosidase, PB, pH 6.5; (d)  $\beta$ -GlcNAcase, PB, pH 6.5; (e) DMC/Et<sub>3</sub>N, ice bath; (f) Herceptin-Fuc $\alpha$ 1,6GlcNAc (**6**), *endo*-S D233Q, Tris buffer, pH 7.4.

**Table 1** Glycoforms and MS data of glycoengineered Herceptin

Entry	Compound	Glycoforms	Calculated mass (Dalton)	Found mass (Dalton)
1	<b>6</b>	Fuc $\alpha$ 1,6GlcNAc	145806.06	145805.35
2	<b>7a</b>	S2G2F	149809.45	149810.52
3	<b>7b</b>	G2F	148645.06	148656.89
4	<b>7c</b>	G0F	147996.85	147997.27
5	<b>7d</b>	Man3GlcNAc2F	147184.54	147185.75
6	<b>14a</b>	Azido-oxime-S2G2F	149897.47	149890.43
7	<b>14b</b>	Azido-amine-S2G2F	149897.62	149906.31
8	<b>14c</b>	Azido-amide-oxime-S2G2F	150181.62	150191.82
9	<b>14d</b>	Alkyne-amide-oxime-S2G2F	150001.49	150002.00
10	<b>14e</b>	Alkyne-oxime-S2G2F	149773.41	149772.38

chemoenzymatic transglycosylation using *in situ* oxazolines. As shown in Scheme 1, *in situ* oxazoline **2** obtained from SGP by successive *endo*-M digestion and DMC/Et<sub>3</sub>N treatment was directly incubated with Herceptin-Fuc $\alpha$ 1,6GlcNAc (**6**) and *endo*-S D233Q in a Tris buffer (pH 7.4). SDS-PAGE monitoring (Fig. 1A) implicated the efficient chemoenzymatic reaction giving product **7a** in nearly complete conversion rate within 30 min. LC-MS analysis (Fig. 1B) of **7a** *via* this one-pot procedure also indicated the homogeneous S2G2F glycoform of the product in both multiple charged and deconvoluted MS spectra. This result demonstrated that the one-pot chemoenzymatic synthesis of glycoengineered IgG could be successfully and efficiently achieved despite the presence of *endo*-M, GlcNAc-hexapeptide, DMC derivative, and triethylamine salts in the reaction buffer. In this case, *endo*-M does not cleave the fucosylated *N*-glycan<sup>68</sup> and thus would not cause the reverse deglycosylation of glycoengineered IgG. Additionally, we noticed that the hydrolytic activity of *endo*-M was completely lost after adding DMC/Et<sub>3</sub>N and barely recovered after the next-step, which involved neutralization of the *in situ* oxazoline with Tris buffer. The GlcNAc-hexapeptide released from SGP

after *endo*-M digestion did not affect the chemoenzymatic reaction because the *endo*-S and its mutants specifically catalyze the IgG Fc fragment other than other GlcNAc-containing substrates.<sup>16</sup> DMC as a coupling reagent raises concern of chemical side-reactions, but in the step of oxazoline formation the majority of DMC was converted to its inactive derivative 1,3-dimethyl-2-imidazolidinone (DMI) in NMR monitoring as reported.<sup>67,69</sup> In our one-pot procedure, there was no cross-linking side-product observed and adding of glycine as the scavenger for DMC into the reaction did not exhibit a difference in the reaction results. Also, the activity of the *endo*-S mutant was not affected in the presence of DMI and triethylamine salts. The data clearly showed that the one-pot strategy for the chemoenzymatic synthesis of glycoengineered IgG was compatible with the reagents used for oxazoline preparation and a single-step purification of the product *via* a protein A affinity column could easily afford the pure glycoengineered IgG.

The non-enzymatic attachment of *N*-glycan oxazoline onto the protein occurred in previous reports<sup>55,69</sup> especially in the case of high-concentration substrates. Therefore, we investigated the non-enzymatic glycation reaction between *in situ* oxazoline **2** and acceptor **6**. Oxazoline **2** in 1.0, 1.5, 2.5, and 5.0 mM was incubated with **6** in the absence of the *endo*-S mutant and monitored by SDS-PAGE after 1 h, 2 h, 3 h, 4 h, and 12 h (Fig. S6†). After 12 h, the non-enzymatic glycation side-products were observed in the reaction under all conditions, however, the higher concentration vial exhibited much more glycation product. Within 3 h, reactions with 1.0, 1.5, and 2.5 mM of **2** caused very few non-enzymatic glycation products. Based on this result, we optimized the one-pot chemoenzymatic reaction conditions using oxazoline in 1.5 mM and performing transglycosylation for 1–2 h to avoid the non-enzymatic side-reactions. The glycoengineered Herceptin products were achieved in high yield under these conditions and the products were further characterized by LC-MS analysis after PNGase-F digestion to ensure the right linkage of target products as discussed below (Fig. 2, 5, and Scheme S1†).

### IgG glycoengineering with non-natural *N*-glycan substrates

The efficient one-pot chemoenzymatic synthesis of glycoengineered IgG enables rapid glycosylation remodeling of mAb using the *N*-glycan precursor SGP directly. With this established approach, we sought to introduce chemical tags on

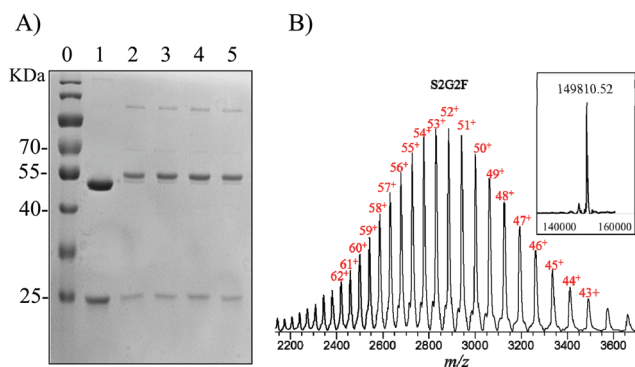


**Fig. 1** SDS-PAGE and LC-MS profiles of glycoengineered Herceptin **7a** *via* one-pot chemoenzymatic synthesis. (A) SDS-PAGE analysis of one-pot chemoenzymatic transglycosylation of Herceptin-Fuc $\alpha$ 1,6GlcNAc (**6**) and *in situ* oxazoline **2** catalyzed by *endo*-S D233Q. Lane 0: marker, Lane 1: Herceptin-Fuc $\alpha$ 1,6GlcNAc (**6**), Lane 2–5: one-pot reaction monitoring after 0.5 h, 1 h, 2 h, and 3 h. (B) LC-MS profile of intact glycoengineered Herceptin **7a**. The multiple charged *m/z* data are labeled with charge numbers. The deconvolution mass spectrum is shown in the embedded box.

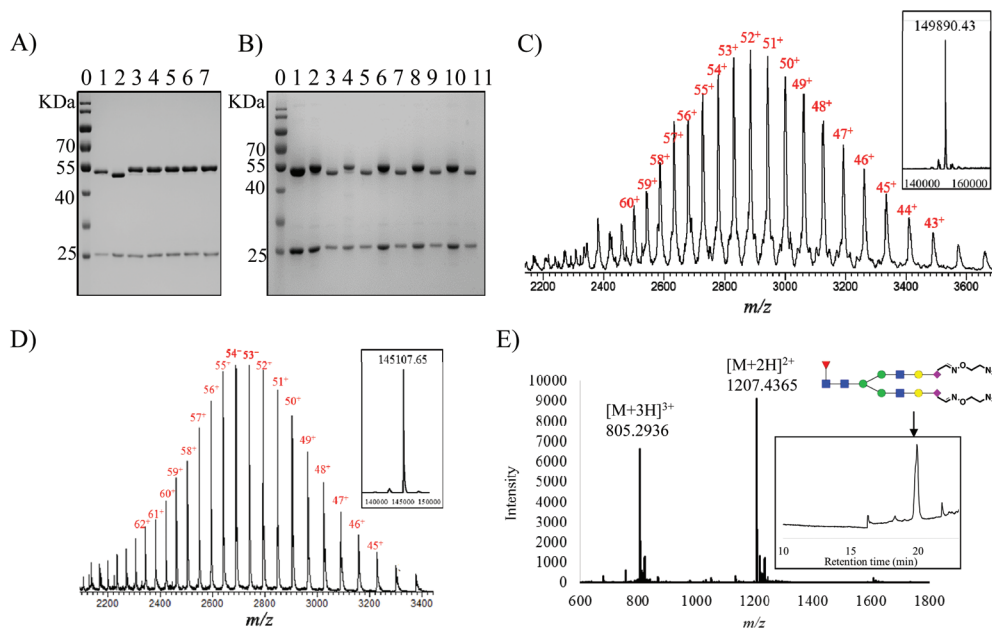


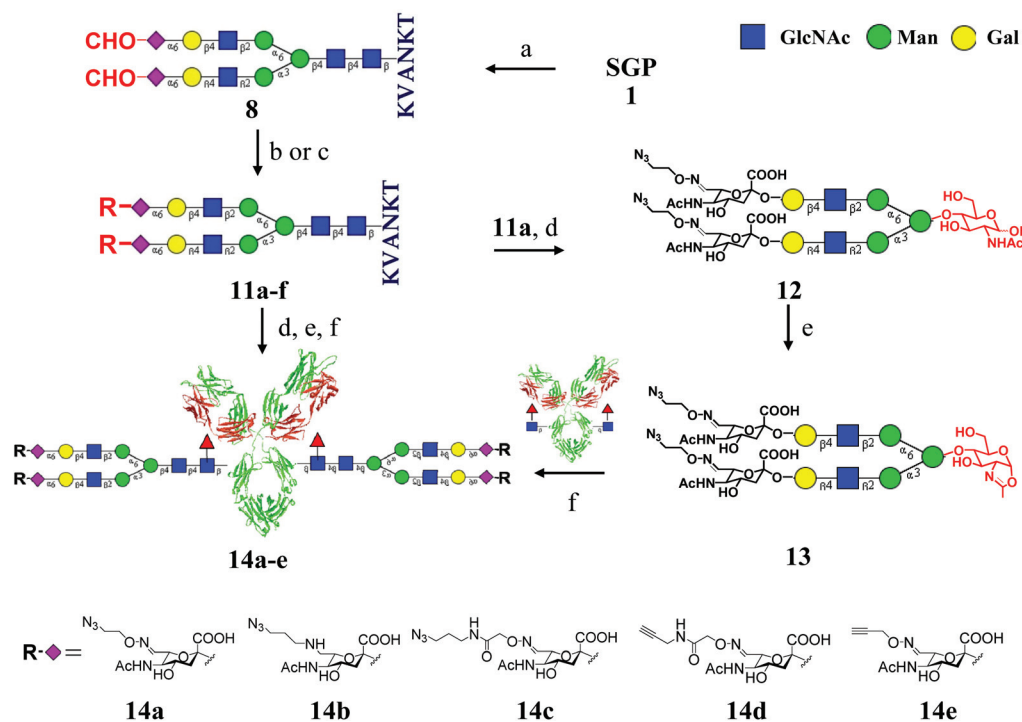
**Fig. 2** SDS-PAGE and LC-MS characterization on glycoengineered Herceptin **14a–e** bearing non-natural *N*-glycans. (A) SDS-PAGE analysis of **14a–e**. Lane 0: marker, Lane 1: commercial Herceptin, Lane 2: Herceptin-Fuc $\alpha$ 1,6GlcNAc (**6**), Lane 3–7, **14a–e**; (B) PNGase-F digestion of **14a–e**. Lane 0: marker, Lane 1: commercial Herceptin, Lane 2, 4, 6, 8, 10: **14a–e**, Lane 3, 5, 7, 9, 11: **14a–e** after PNGase-F digestion; (C) LC-MS profiles of **14a**. The multiple charged *m/z* data are labeled with charge numbers. The deconvolution mass spectrum is shown in the embedded box. (D) LC-MS profiles of Herceptin-Asp<sup>297</sup> resulted from PNGase-F-treated **14a**. (E) MS profile of the released glycan **28** from **14a** by PNGase-F digestion. The ion flow chromatography of the PNGase-F digested sample is shown in the embedded box and the peak of **28** is marked with an arrow.

IgG glycans by non-natural glycan substrates for site-specific conjugation. To test this idea, we synthesized a series of modified SGPs as the precursors of glycan donors. As shown in Scheme 2, SGP (**1**) was treated with NaIO<sub>4</sub> to oxidize the triol of sialic acid motifs giving the CHO-SGP (**8**). With the aldehyde function group, azido or alkyne tags were easily assembled onto **8** *via* reductive amidation with amines (**9a–b**) or oxime formation with hydroxylamines (**10a–d**). Three azido-SGPs (**11a–c**) and three alkyne-SGPs (**11d–f**) were prepared for further glycoengineering of Herceptin. Characterization of **11a–f** with NMR, MS, and HPLC is provided in the ESI.†

To investigate the substrate tolerance of the *endo-S* enzyme on these sialyl modifications, we chose the azido-SGP **11a** as the starting material and synthesized the corresponding *N*-glycan oxazoline **13** by a similar procedure described above. *endo-M* digestion of **11a** released the azido *N*-glycan **12** which was purified by semi-preparative HPLC. **12** was converted to its oxazoline form **13** and subjected to gel-filtration purification through a Sephadex G-25 column. The assignments on the NMR spectra of **12** and **13** are available in the Experimental section and ESI.† With azido *N*-glycan oxazoline **13** in hand, we performed the chemoenzymatic transglycosylation with Herceptin-Fuc $\alpha$ 1,6GlcNAc (**6**) catalyzed by *endo-S* D233Q. The result indicated that the *endo-S* mutant recognized the azido-tagged oxazoline **13** as the same as the native *N*-glycan oxazoline **2** and afforded the azido-Herceptin **14a** in a quantitative yield within 1 h. MS analysis of intact **14a** showed the deconvoluted mass of 149 890.43 (Fig. 2B) which was in agreement with the calculated mass.

Next, we applied the one-pot method for chemoenzymatic transglycosylation of Herceptin with these non-natural glycan substrates. The *in situ* oxazoline **13** derived from azido-SGP **11a** was directly incubated with Herceptin acceptor **6** and the *endo-S* mutant in a Tris buffer. SDS-PAGE monitoring and LC-MS detection (Fig. S7†) indicated that product **14a** was obtained efficiently in a quantitative conversion rate after one hour. To test whether the non-enzymatic glycation took place simultaneously, we performed glycan analysis of **14a** by PNGase-F digestion. Chemoenzymatic transglycosylation catalyzed by the *endo-S* mutant assembles the *N*-glycan onto the first GlcNAc on IgG Fc Asn<sup>297</sup> *via* a beta 1,4 linked glycosidic bond, whereas the non-enzymatic glycation takes place randomly on the amino acids of protein. PNGase-F cleaves the amide bond between the nitrogen of the *N*-glycan reducing end and the side-chain carbonyl of glycosite Asn, and then releases the intact *N*-glycan and converts the Asn to Asp (Scheme S1†). Therefore, the enzymatic product will be deglycosylated by PNGase-F and the non-enzymatic side-product will not. As shown in SDS-PAGE of Fig. 2B, the heavy-chain band of PNGase-F-treated **14a** totally shifted to a downside position suggesting the complete release of *N*-glycan, and there was no non-enzymatic glycation observed. Furthermore, LC-MS analysis of the resulting Herceptin-Asp<sup>297</sup> (Fig. 2C) and azido-*N*-glycan **28** (Fig. 2D) clearly verified the enzymatic product that linked the *N*-glycan onto the GlcNAc motif of **6** but not onto the amino acid residues.

The successful one-pot glycoengineering of Herceptin with azido-tagged SGP demonstrated the broad substrate specificity



**Scheme 2** Conditions: (a)  $\text{NaIO}_4$ , ice bath; (b) 3-azido-1-propanamine (9a) or propargylamine (9b)/ $\text{NaCNBH}_3$ , phosphate buffer, pH 6.0; (c) hydroxylamine 10a–d (see the ESI<sup>†</sup>), PB, pH 7.5; (d) *endo*-M, PB, pH 6.5; (e) DMC/ $\text{Et}_3\text{N}$ ; (f) 6, *endo*-S D233Q, Tris buffer, pH 7.4.

of the *endo*-S mutant with extensive tolerance on sialyl modification of biantennary complex-type *N*-glycans. We then tested the other four non-natural *N*-glycan substrates 11b–11e bearing diverse linker fragments for one-pot glycoengineering. The SDS-PAGE monitoring and LC-MS analysis on intact glycoengineered products are illustrated in the ESI (Fig. S8–S11<sup>†</sup>). The SDS-PAGE of purified products 14b–e is summarized in Fig. 2A, and PNGase-F digestion of each glycoengineered Herceptin indicated no non-enzymatic side-product in SDS-PAGE detection (Fig. 2B). All five non-natural *N*-glycan substrates suggested similar efficiency in one-pot glycoengineering of Herceptin. With this method, we can easily label the *N*-glycan of IgG for site-specific conjugation.

#### Glycosite-specific antibody–drug conjugations *via* the tagged-glycoforms of IgG

Azido or alkyne-tagged Herceptin 14a–e enable the small-molecule conjugation *via* the azide–alkyne Huisgen cycloaddition, also known as “click chemistry”. We initiated the conjugation with copper-catalyzed click reaction using alkyne-Herceptin 14d–e and azido-propanamine (9a) as the model materials. Under catalytic conditions of  $\text{CuSO}_4$ , L-ascorbic acid, and ligand BTAA,<sup>70</sup> the click reaction did not proceed smoothly. Precipitation of the IgG protein was observed in the reaction system and LC-MS monitoring showed a low conversion rate. Then, we turned to the strain-promoted copper-free approach using cyclooctyne reagents<sup>71–73</sup> for enhanced click reactions. Dibenzocyclooctyne (DBCO) was assembled on small molecules such as toxin DM1 (15) and MMAE (16), or

fluorescent tag Cy5 (19) to give the corresponding DBCO-tagged compounds 21a–d (see the Experimental section and ESI<sup>†</sup> for chemistry details). Using the azido-Herceptin (14a) and DBCO-MCC-DM1 (21a) as the substrates, we performed the copper-free click reaction in a phosphate buffer (pH 7.5) containing 10% DMSO and synthesized the site-specific ADC 22a. The cycloaddition conjugation was accomplished efficiently as monitored by SDS-PAGE and LC-MS (Fig. 3A and 4A). SDS-PAGE analysis of 22a showed its heavy-chain band in a higher position than 14a but light-chain bands of both samples remained in the same size, suggesting that the gained mass by toxin conjugation was site-specific on the heavy chain. LC-MS verified the successful conjugation of totally four DM1 moieties on the four azido groups of two Fc *N*-glycans.

Glycosite-specific ADCs with diverse linker fragments were synthesized following the same strategy. Azido-oxime-Herceptin (14a) and azido-amine-Herceptin (14b) were conjugated with other two DBCO-tagged toxins 21b and 21c bearing a cleavable Val-Cit dipeptide and/or a poly(ethylamine) (PEG) motif. Corresponding ADCs 22b–d were obtained and the increased mass by conjugation was confirmed by SDS-PAGE (Fig. 3B and C) and LC-MS (Fig. 4B–E). The MS data and linker information of these site-specific ADCs are also summarized in Table 2. To validate the site-specific conjugation, 22a–c were treated with PNGase-F for deglycosylation. Fig. 5A shows the heavy-chain bands of all three ADCs reduced to the lower position as the same level as deglycosylated commercial Herceptin. LC-MS measurements on the released glycan–drug complex 29 displayed a series of charged *m/z* data in high accordance with

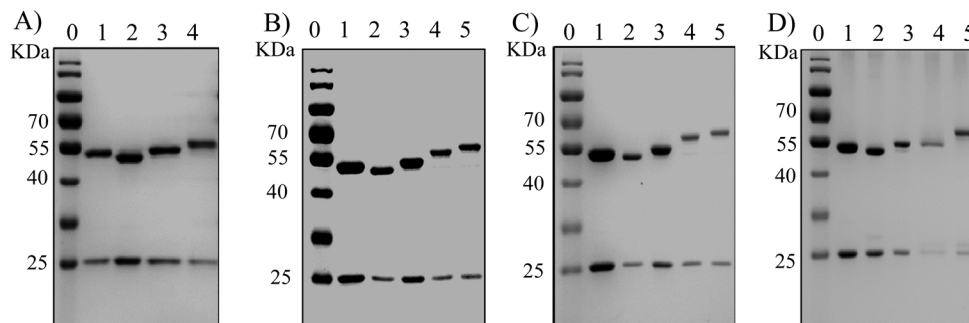


**Fig. 3** SDS-PAGE profiles of site-specific ADCs. (A) ADC 22a. Lane 0: marker, Lane 1: commercial Herceptin, Lane 2: Herceptin 6, Lane 3: Herceptin 14a, Lane 4: ADC 22a. (B) ADCs 22b and 22c. Lane 0: marker, Lane 1: commercial Herceptin, Lane 2: Herceptin 6, Lane 3: Herceptin 14a, Lane 4: ADC 22b, Lane 5: ADC 22c. (C) ADCs 22d and 22e. Lane 0: marker, Lane 1: commercial Herceptin, Lane 2: Herceptin 6, Lane 3: Herceptin 14a, Lane 4: ADC 22d, Lane 5: ADC 22e. (D) ADCs 23 and 24. Lane 0: marker, Lane 1: commercial Herceptin, Lane 2: Herceptin 6, Lane 3: Herceptin 14a, Lane 4: ADC 23, Lane 5: ADC 24.

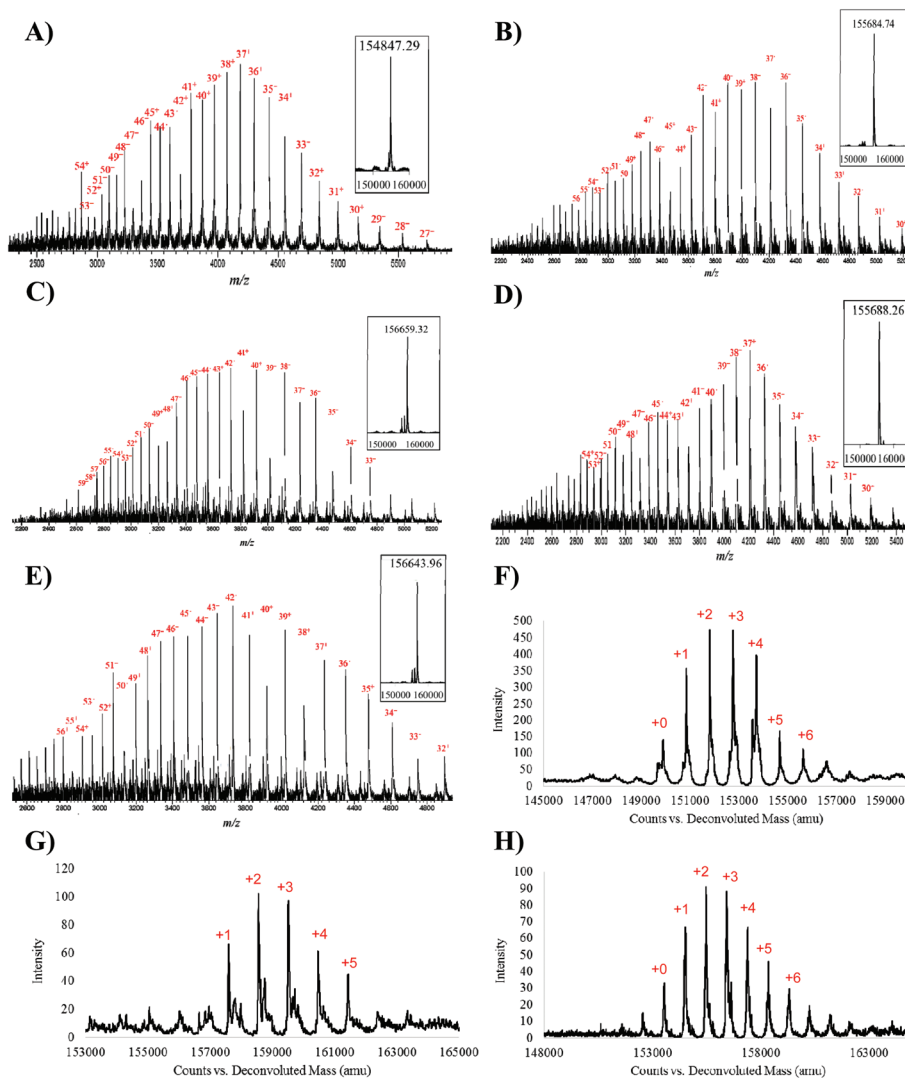


**Fig. 4** Mass spectra of site-specific ADCs. (A) ADC 22a. The multiple charged  $m/z$  data are labeled with charge numbers. The deconvolution mass spectrum is shown in the embedded box. (B) ADC 22b. (C) ADC 22c. (D) ADC 22d. (E) ADC 22e. (F) The deconvolution mass spectrum of Lys-conjugated ADC 23. The conjugation number of DM1 for each detected mass was assigned and marked with red-colored numbers. (G) The deconvolution mass spectrum of dual-drug ADC 24. (H) The deconvolution mass spectrum of 25 bearing Lys-conjugated DM1 and glycan-labeled Cy5.

**Table 2** Chemical profiles and antitumor activities of ADC samples

Entry	ADCs	Precursors	Glycosite linkers	Payload	DAR <sup>b</sup>	Found mass	EC <sub>50</sub> <sup>g</sup>
1	<b>T-DM1</b>		MCC (on Lys)	DM1	3.2	Multi-mass <sup>d</sup>	0.06
2	<b>T-MMAE</b>		MCC (on Lys)	MMAE	3.5	Multi-mass <sup>d</sup>	0.15
3	<b>22a</b>	<b>14a</b>	DBCO-MCC	DM1	4	154847.29	>10
4	<b>22b</b>	<b>14a</b>	DBCO-PEG <sub>4</sub>	DM1	4	155684.74	>10
5	<b>22c</b>	<b>14a</b>	DBCO-PEG <sub>4</sub> -VC-PAB	MMAE	3.8 <sup>c</sup>	156659.32	0.09
6	<b>22d</b>	<b>14b</b>	DBCO-PEG <sub>4</sub>	DM1	4	155688.26	>10
7	<b>22e</b>	<b>14b</b>	DBCO-PEG <sub>4</sub> -VC-PAB	MMAE	3.8 <sup>c</sup>	156643.96	ND
8	<b>23</b>	<b>14a</b>	MCC (on Lys)	DM1	2.6	Multi-mass <sup>e</sup>	ND
9	<b>24<sup>a</sup></b>	<b>23</b>	MCC (on Lys) DBCO-PEG <sub>4</sub> -VC-PAB	DM1 MMAE	2.6 3.8 <sup>c</sup>	Multi-mass <sup>f</sup>	0.06

<sup>a</sup> Dual-drug ADC **24** contains DM1 conjugated on Lys residues and MMAE conjugated on glycans with two DAR values. <sup>b</sup> The DAR values are calculated based on the intensity percentage of each found mass of ADC in the MS spectra. <sup>c</sup> DBCO-PEG<sub>4</sub>-VC-MMAE **21c** used in preparation of these ADCs contained a small quantity of the DBCO fragment without MMAE and caused the DAR reduction. <sup>d</sup> See the ESI. <sup>e</sup> The found multiple mass in deconvolution data: 149907.63 (+0 DM1), 147719.04 (+1 DM1), 151823.00 (+2 DM1), 152786.70 (+3 DM1), 153734.55 (+4 DM1), 154696.10 (+5 DM1). <sup>f</sup> The found multiple mass in deconvolution data: 157606.71 (+1 DM1), 158566.82 (+2 DM1), 159530.22 (+3 DM1), 160477.23 (+4 DM1), 161446.46 (+5 DM1). <sup>g</sup> The EC<sub>50</sub> values (μg mL<sup>-1</sup>) of antitumor activity are calculated based on the cytotoxicity assay with the SK-BR-3 cell line. ND: not detected.

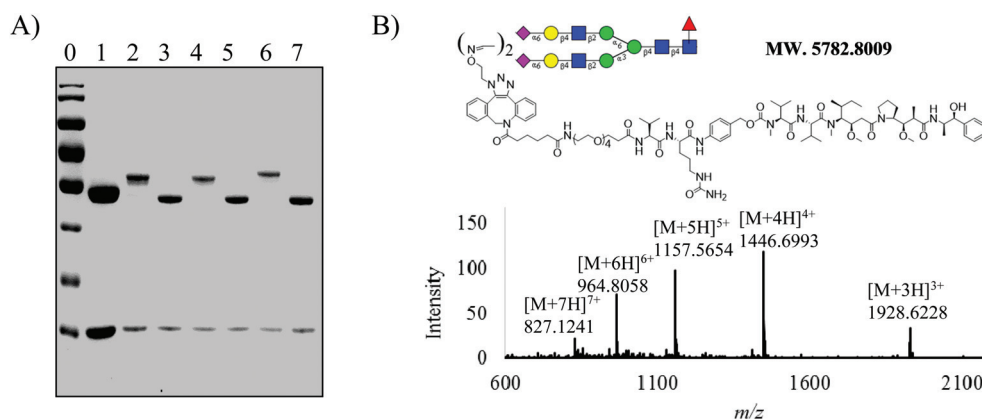


**Fig. 5** SDS-PAGE and LC-MS analysis of site-specific ADCs after PNGase-F digestion. (A) SDS-PAGE of ADCs **22a–c** treated with PNGase-F. Lane 0: marker; Lane 1: commercial Herceptin; Lane 2, 4, 6: **22a**, **22b**, **22c**; Lane 3, 5, 7: **22a**, **22b**, **22c** after PNGase-F digestion. (B) HR-MS profile of the released glycan-drug moiety **29** from ADC **22c**.

the calculated molecular weight (Fig. 5B). These data solidly demonstrated that the glycosite-specific conjugation method was successfully applied in ADC preparation with diverse linker structures.

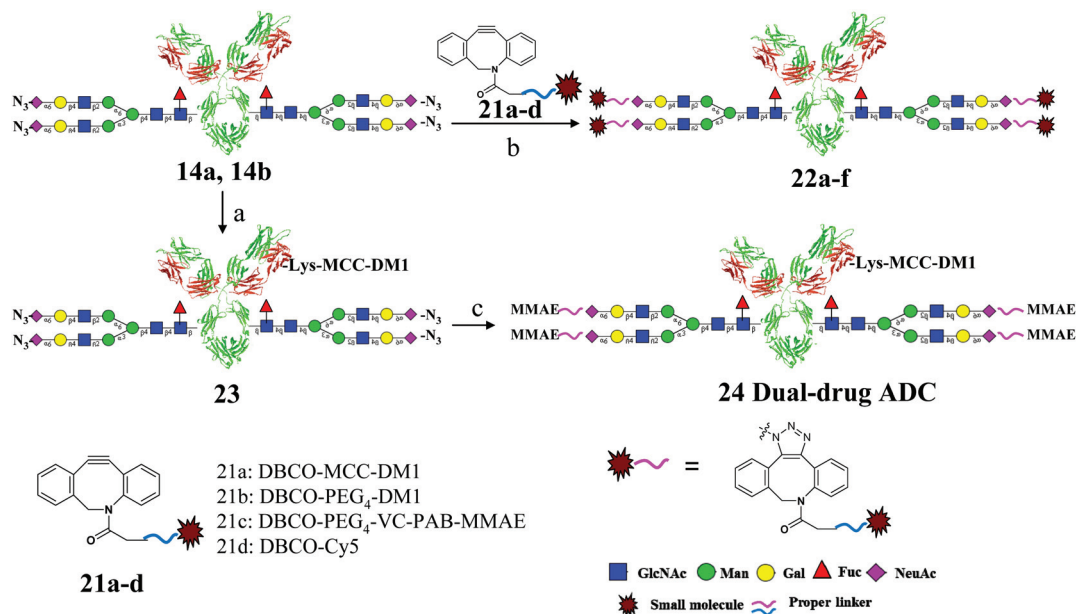
Furthermore, combining this glycosite-specific conjugation and conventional random conjugation, we developed a dual-payload strategy for ADC design by assembly of one payload (MMAE) on glycans and another different payload (DM1) on Lys residues. As shown in Scheme 3, azido-Herceptin **14a** was treated with DM1-SMCC (**20**) bearing an active carboxylic succinimide for Lys conjugation, to give the random linked ADC **23** carrying azido-tagged glycans. Then, DBCO-PEG<sub>4</sub>-VC-MMAE (**21c**) was introduced on the azido groups of **23** via click reaction and afforded dual-drug ADC **24**. The SDS-PAGE analysis (Fig. 3D) of **23** and **24** indicated the smeared bands of both heavy chains and light chains because of the random conjugation. The LC-MS spectra (Fig. 4F and G) of **23** and **24** displayed the mixture mass of ADC carrying different numbers of payloads. The drug-antibody ratio (DAR) was calculated based

on the intensity percentage of each found mass in all deconvolution data. Dual-drug ADC **24** has two DARs: DAR of DM1 on Lys residues was 2.6 as the same as **23**; DAR of MMAE on glycans was 3.8 (Table 2).

The azido-tagged IgG also enables site-specific labeling with fluorescent reagents. DBCO-Cy5 (**21d**) was linked to the azido-glycan of **14a** giving site-specific Cy5-labeled Herceptin **22f** (Fig. S12†). This label could be applied in conventional ADC as well. Random linked ADC **23** bearing azido moieties on glycans was labeled with **21d** and afforded site-specific Cy5-labeled ADC **25** (Fig. 4H). Fluorescent labeling of IgG or ADC on *N*-glycans represents another functionalization application of chemoenzymatic glycoengineering with non-natural glycan substrates.

### Biological assays with site-specific conjugates

The advantage of site-specific conjugation is to avoid the possible influence on the antigen-binding domain by random ligation. We tested the antigen-binding activity of commercial



**Scheme 3** Conditions: (a) DM1-SMCC (20), phosphate buffer, pH 7.5; (b) 21a–d, PB, pH 7.5; (c) 21c, PB, pH 7.5.

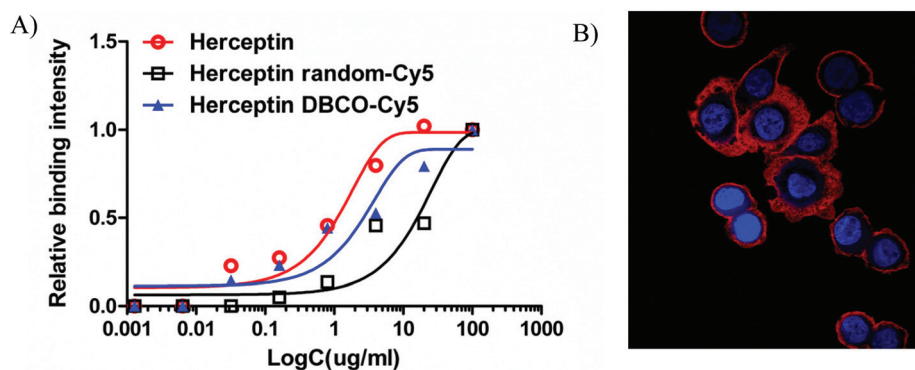


**Fig. 6** Cell-based antigen binding properties of Cy5-labeled Herceptin. (A) SK-BR-3 cell-based ELISA assay of commercial Herceptin (red), site-specific conjugate Herceptin-Cy5 (22f) (blue), and random conjugate Herceptin-Cy5 (26) (black); (B) SK-BR-3 cell binding assay with site-specific conjugate Herceptin-Cy5 (22f) by using a confocal microscope. The nucleus is labeled in blue and Cy5-labeled Herceptin on the cell surface is displayed in red.

Herceptin, random-labeled Herceptin-Cy5 (26) and glycosite-specific Cy5-labeled Herceptin (22f) by cell-based ELISA. A HER2-positive breast cancer cell line, SK-BR-3, was coated on a plate and these three Herceptin samples were measured for the binding affinity against the coated target cell. As shown in Fig. 6A, the K<sub>D</sub>s of commercial Herceptin, 22f, and 26 were 1.2, 3.5, and 24 μg mL<sup>-1</sup> respectively. Apparently, random conjugation caused significant reduction on antigen-binding activity compared with the site-specific conjugation. In addition, we examined the target cell attachment of site-specific labeled Herceptin 22f by confocal microscopy (Fig. 6B). SK-BR-3 cells were incubated with 22f at 4 °C for 30 min and then subjected to confocal imaging. Fluorescence detection based on Cy5 label indicated that the antibody was crowded on the cell surface. These data demonstrated that the

site-specific labeling of IgG enabled by glycoengineering is an optimal strategy for imaging without affecting the antigen binding properties.

Cytotoxicity assay against the cancer cell line SK-BR-3 was carried out with glycosite-specific ADCs. For comparison, we also synthesized the random Lys conjugate T-DM1 and T-MMAE (see the ESI†). As shown in Fig. 7 and Table 2, T-DM1 and T-MMAE indicated potent antitumor activity with the EC<sub>50</sub> values of 0.06 and 0.15 μg mL<sup>-1</sup>, while ADCs 22a, 22b, and 22d did not affect the cell proliferation besides the efficacy of the antibody itself. However, ADCs 22c and 24 inhibited the cancer cell growth as efficiently as T-DM1 with the EC<sub>50</sub> values of 0.09 and 0.06 μg mL<sup>-1</sup>. These data elucidated the importance of a linker fragment for glycosite-specific ADCs. Based on these results, the cleavable Val-Cit motif is crucial for

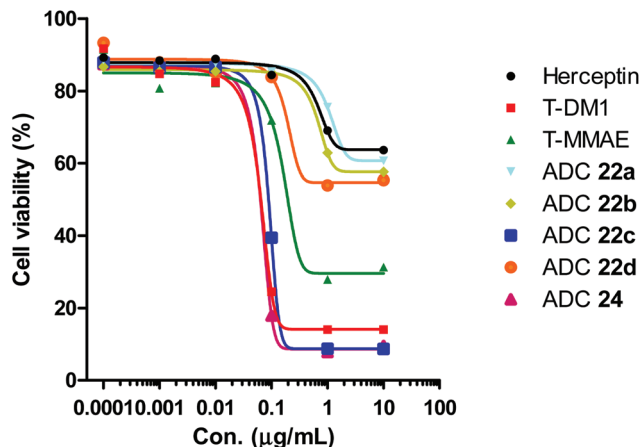


Fig. 7 Cytotoxicity assay of ADC samples on a HER2-positive cell line, SK-BR-3.

site-specific ADCs but not for Lys-conjugated ADCs to release the toxin after cell endocytosis. The endocytosed T-DM1 was digested in lysosome to give DM1-MCC-Lys as the cytotoxic agent. For glycan-conjugated ADCs, this mechanism does not seem to be effective probably due to the hindrance of large *N*-glycan by releasing toxins. Even with a cleavable handle of oxime, the ADCs 22a and 22b did not show antitumor cytotoxicity. Whereas, 22c and 24 carrying the Val-Cit fragment as a protease substrate successfully achieved cancer cell inhibition. The glycosite-specific ADCs required a different releasing mechanism that could guide us for ADC design in future. The dual-drug ADC 24 at a lower DM1 DAR (2.6) indicated the same antitumor activity as T-DM1 (DAR 3.2) that may be due to the partial contribution of MMAE to 24. Since DM1 and MMAE target the cancer cell tubulin in a similar mechanism, dual-drug ADCs with two different toxic agents such as combined anti-tubulin and DNA-damaging toxins are more attractive for future research and development.

## Conclusion

An efficient one-pot chemoenzymatic glycoengineering approach was established for IgG Fc glycosylation remodeling directly using an egg-yolk sialylglycopeptide (SGP) or its non-natural derivatives carrying azido or alkyne tags. This approach enables the rapid synthesis of functionalized therapeutic IgG antibodies for glycosite-specific conjugation with small-molecule drugs or fluorescent agents. Site-specific ADCs and dual-drug ADCs were developed based on this strategy.

## Experimental section

### Materials

*endo*-M, *endo*-S wild type, *endo*-S mutant D233Q and PNGase-F were expressed in *E. coli* following the reported procedure<sup>16,65</sup>

(see the ESI†).  $\beta$ -1,4-Galactosidase was purchased from New England Biolabs (Ipswich, MA). Neuraminidase and  $\beta$ -*N*-acetylglucosaminidase were purchased from Sigma-Aldrich (Shanghai, China). Sialylglycopeptide (1) was extracted and purified from egg yolk powder following the literature<sup>54</sup> (see the ESI†). 3-Azido-1-propanamine (9a), propargylamine (9b), and HPLC grade acetonitrile was purchased from J&K Chemical Ltd (Shanghai, China). Syntheses of hydroxylamine compounds 10a–d are described in the ESI.† DM1 (15) and MMAE (16) were purchased from Levena Biopharma (Nanjing, China). Dibenzocyclooctyne (DBCO)-amine (17) and DBCO-PEG<sub>4</sub>-acid (18) were purchased from Sigma-Aldrich (Shanghai, China). Sulfo-cyanine5 NHS ester (19) was purchased from Little-PA Sciences Co., Ltd (Wuhan, China). Syntheses of drug-linker intermediates 20, and 21a–d are described in the ESI.† Porous graphite carbon (PGC) cartridges (Hypercarb) were purchased from Thermo Fisher Scientific (Beijing, China). Other chemical reagents and solvents were purchased from Sinopharm Chemical Reagent Co. (Shanghai, China) or Sigma-Aldrich (Shanghai, China) and used without further purification. Nuclear magnetic resonance (NMR) spectra were measured on a Varian-MERCURY Plus-400 or 500 instrument. ESI-HRMS spectra were measured on an Agilent 6230 LC-TOF MS spectrometer.

### High performance liquid chromatography (HPLC)

**Method A:** Analytical RP-HPLC was performed on a Beijing ChuangXinTongHeng LC3000 (analytic) instrument with a C18 column (5  $\mu$ m, 4.6  $\times$  150 mm) at 40  $^{\circ}$ C. The column was eluted with a linear gradient of 2–90% acetonitrile containing 0.1% TFA for 30 min at a flow rate of 1 mL min<sup>-1</sup>. **Method B:** Analytical RP-HPLC was performed on a Beijing ChuangXinTongHeng LC3000 (analytic) instrument with a C18 column (5  $\mu$ m, 4.6  $\times$  150 mm) at 40  $^{\circ}$ C. The column was eluted with a linear gradient of 2–11% acetonitrile containing 0.1% TFA for 10 min and then 11–90% acetonitrile for an additional 20 min at a flow rate of 1 mL min<sup>-1</sup>. **Method C:** Analytical RP-HPLC was performed on a Thermo ultimate 3000 instrument with a column (5  $\mu$ m, 4.6  $\times$  250 mm) at 40  $^{\circ}$ C. The column was eluted with a linear gradient of 2–90% acetonitrile containing 0.1% TFA for 30 min at a flow rate of 1 mL min<sup>-1</sup>. **Method D:** Preparative HPLC was performed on a Beijing ChuangXinTongHeng LC3000 (preparative) instrument with a preparative column (Waters, C18, OBD, 5  $\mu$ m, 19  $\times$  250 mm). The column was eluted with a suitable gradient of aqueous acetonitrile containing 0.1% TFA at a flow rate of 10 mL min<sup>-1</sup>.

### Liquid chromatography mass spectrometry (LC-MS)

ESI-MS spectra were measured on an Agilent 6230 LC-TOF MS spectrometer. The small molecules were analyzed using a short guard column and eluted with 70% methanol containing 0.1% formic acid. The mass spectra of small molecules were recorded in the mass range of 200–3000 or 600–2000 under a high resolution mass-spec mode (HRMS, standard 3200 *m/z*, 4 GHz). Key source parameters: a drying nitrogen gas flow of

11 L min<sup>-1</sup>; a nebulizer pressure of 40 psi; a gas temperature of 350 °C; a fragmenter voltage of 175 V; a skimmer voltage of 65 V; and a capillary voltage of 4000 V. The antibodies and ADCs were measured with an Agilent C-18 column (3.5 μm, 50 × 2.1 mm) at 55 °C. The column was eluted with an isocratic gradient of 5% acetonitrile (Buffer B) and 95% water containing 0.1% formic acid (Buffer A) in the first 10 min, a linear gradient of 5–95% acetonitrile for an additional 10 min and an isocratic gradient of 95% acetonitrile for another 10 min at a flow rate of 0.2 mL min<sup>-1</sup>. The mass spectra of antibodies were performed under the extended mass range mode (high 20 000 *m/z*, 1 GHz) and the data were collected in the mass range of 800–5000. Key source parameters: a drying nitrogen gas flow of 11 L min<sup>-1</sup>; a nebulizer pressure of 60 psi; a gas temperature of 350 °C; a fragmenter voltage of 400 V; a skimmer voltage of 65 V; and a capillary voltage of 5000 V. The multiple charged peaks of the antibody were deconvoluted using the Agilent MassHunter Bioconfirm software (deconvolution for protein, Agilent technology) with the deconvolution range from 100 kDa to 200 kDa; other parameters were set at default values for protein deconvolution. The TOF was calibrated over the range 0–5000 *m/z* using Agilent ESI calibration mix solution before analysis. The peak of MS 922 is the internal standard for calibration.

#### High-performance anion exchange chromatography with pulsed amperometric detection (HPAEC-PAD)

The HPAEC-PAD analysis was performed on an ICS 5000<sup>+</sup> system (Thermo Scientific) with a PA100 anion exchange column (4 × 250 mm) and a guard column (4 × 50 mm) at 40 °C. The column was eluted with 100 mM sodium hydrate solution (Sigma) for the first 2 min and a linear of 0–150 mM sodium acetate (Sigma) in 100 mM sodium hydrate for an additional 20 min at a flow rate of 1 mL min<sup>-1</sup>.

#### General procedure for one-pot semi-synthesis of *N*-glycan oxazoline substrates (2–5)

A solution of sialylglycopeptide **1** (100 mg) in phosphate buffer (PB, 50 mM, pH 6.25, 1 mL) was incubated with *endo*-M (0.5 mg) at 30 °C and monitored by RP-HPLC (Method B). The sialoglycan in the reaction mixture was then transformed into sialoglycan-oxazoline **2** with the addition of 2-chloro-1,3-dimethylimidazolidinium chloride (DMC, 15 eq.) and trimethylamine (Et<sub>3</sub>N, 45 eq.). For exoglycosidase digestion, the reaction mixture was incubated with additional neuraminidase and/or β 1,4-galactosidase and/or β-*N*-acetylglucosaminidase. The reaction was monitored by HPAEC until complete deglycosylation, then DMC (15 eq.) and Et<sub>3</sub>N (45 eq.) was added. Oxazolines **3**, **4** and **5** were obtained after solid-phase extraction *via* a porous graphite carbon (PGC) column and gel-filtration *via* a Sephadex G-25 column. The NMR spectra of the oxazolines synthesized from the one-pot strategy were consistent with the reported data.<sup>16,54,61</sup> NMR and HPAEC-PAD spectra are available in the ESI.†

#### CHO-SGP (8)

To a stirred solution of SGP **1** (100 mg) in PB (0.2 M, pH 7.1, 5 mL) in an ice bath, aqueous sodium periodate (30 mM, 5 mL) was added. The reaction mixture was stirred and protected from light for 15 min and was then subjected to gel-filtration *via* a Sephadex G-25 column. The column was eluted with water and the fractions containing the product were combined and lyophilized to give **8** as a white powder (90.0 mg, yield 94%). <sup>1</sup>H NMR (500 MHz, deuterium oxide) δ 5.05 (1H, s, H1c), 4.96 (1H, d, *J* = 9.7 Hz, H1a'), 4.88 (3H, m, H1c', H of CHO –C(H)–(OH)<sub>2</sub>), 4.70 (1H, s, H1b), 4.60 (1H, t, *J* = 6.7 Hz, Asn Hα), 4.53 (3H, d, *J* = 7.4 Hz, H1a, H1d, H1d'), 4.39 (1H, d, *J* = 3.5 Hz, Thr Hα), 4.37 (1H, d, *J* = 2.5 Hz, H1e), 4.35–4.27 (3H, m, H1e', Thr Hβ, Lys Hα), 4.24 (1H, q, *J* = 7.1 Hz, Ala Hα), 4.17 (1H, s, H2b), 4.12 (1H, d, *J* = 3.4 Hz, H2c), 4.08 (1H, d, *J* = 7.5 Hz, Val Hα), 4.03 (1H, d, H2c'), 3.99 (3H, t, *J* = 6.4 Hz, Lys Hα, 2H), 2.92 (m, 4H, Lys He), 2.82–2.59 (2H, m, Asn Hβ), 2.51 (2H, dd, *J* = 12.7, 4.2 Hz, H3f<sub>eq</sub>, H3f'<sub>eq</sub>), 2.09–1.88 (19H, m, 6 × 3 Ac, Val Hβ), 1.82 (6H, m, Lys Hβ, H3f<sub>ax</sub>, H3f'<sub>ax</sub>), 1.75–1.56 (4H, m, *J* = 7.5 Hz, Lys Hδ), 1.36 (4H, m, Lys Hγ), 1.30 (3H, d, *J* = 7.5 Hz, Ala Hβ), 1.12 (3H, *J* = 6.5 Hz, Thr Hγ), 0.89 (6H, d, 7.0 Hz, Val Hγ). HSQC ((<sup>1</sup>H, 500 MHz)/(<sup>13</sup>C, 126 MHz), deuterium oxide) 5.05/100.10 (H1c/C1c), 4.96/78.91 (H1a'/C1a'), 4.88/89.17 (H1g/C1g), 4.87/97.65 (H1c'/C1c'), 4.70/101.14 (H1b/C1b), 4.59/50.77 (Hα Asn/Cα Asn), 4.53/100.41 (H1a/C1a, H1d/C1d, H1d'/C1d'), 4.38/58.86 (Hα Thr/Cα Thr), 4.37/104.22 (H1e/C1e, H1e'/C1e'), 4.33/54.21 (Hα Lys/Cα Lys), 4.31/67.76 (Hβ Thr/Cβ Thr), 4.23/50.13 (Hα Ala/Cα Ala), 4.17/71.26 (H2b/C2b), 4.11/77.18 (H2c/C2c), 4.07/60.15 (Hα Val/Cα Val), 4.03/76.82 (H2c'/C2c'), 3.99/53.60 (Hα Lys/Cα Lys), 2.92/39.73 (He Lys/Ce Lys), 2.66/37.45 (Hβ Asn/Cβ Asn), 2.51/40.00 (H3f/C3f, H3f'/C3f'), 2.00/31.01 (Hβ Val/Cβ Val), 1.83/31.01 (Hβ Lys/Cβ Lys), 1.69/39.96 (H3f/C3f, H3f'/C3f'), 1.61/26.93 (Hδ Lys/Cδ Lys), 1.37/22.00 (Hγ Lys/Cγ Lys), 1.30/17.37 (Hβ Ala/Cβ Ala), 1.12/19.63 (Hγ Thr/Cγ Thr), 0.89/19.33 (Hγ Val/Cγ Val). HRMS, calculated for C<sub>108</sub>H<sub>177</sub>N<sub>15</sub>O<sub>66</sub> [M + 3H]<sup>3+</sup> 914.3730, found 914.3734; [M + H<sub>2</sub>O + 3H]<sup>3+</sup> 920.3765, found 920.3787.

#### General Procedure for synthesis of non-natural oxime-SGPs (11a, 11c, 11d, and 11e)

To a solution of **8** (10 mg, 3.65 μmol, 1.0 eq.) in PB (50 mM, pH 7.5, 100 μL) was added **10a–d** (14.6 μmol, 4.0 eq.). The mixture was stirred at room temperature for 2 hours and monitored by RP-HPLC (Method B). The residue was subjected to semi-preparative HPLC purification to give the oxime SGPs **11a**, **11c**, **11d**, and **11e** respectively.

**Azido oxime SGP (11a).** Yield 92.3%. <sup>1</sup>H NMR (500 MHz, deuterium oxide) δ 7.41 (1.6H, dd, *J* = 7.2, 3.3 Hz, H1 of oxime), 6.85 (0.4H, dd, *J* = 6.7, 2.6 Hz, H1 of oxime), 5.07 (1H, s, H1c), 4.96 (1H, d, *J* = 9.6 Hz, H1a'), 4.96 (0.4 H, H6f, H6f'), 4.88 (1H, s, H1c'), 4.76 (1H, s, H1b), 4.59 (1H, t, Asn Hα), 4.53 (3H, d, *J* = 6.7 Hz, H1a, H1d, H1d'), 4.39 (1H, d, *J* = 3.5 Hz, Thr Hα), 4.37 (1H, d, *J* = 2.5 Hz, H1e), 4.35 (1H, d, *J* = 3 Hz, H1e'), 4.34–4.28 (2H, m, Lys1 Hα, Thr Hβ), 4.24 (1H, q, *J* = 7 Hz, Ala Hα), 4.17 (5H, m, H2b, H2 of oxime), 4.17 (1.6H, m, H6f, H6f'),

4.12 (1H, d,  $J = 2$  Hz, H2c), 4.08 (1H, d,  $J = 8$  Hz, Val H $\alpha$ ), 4.04 (1H, d,  $J = 2$  Hz, H2c'), 3.99 (1H, t,  $J = 6.5$  Hz, Lys2 H $\alpha$ ), 2.92 (4H, q,  $J = 7.5$  Hz, Lys H $\epsilon$ ), 2.81–2.61 (2H, m, Asn H $\beta$ ), 2.61–2.51 (2H, dd,  $J = 12.5$  Hz, 2.5 Hz, H3f<sub>eq</sub>, H3f'<sub>eq</sub>), 2.03–1.88 (19H, m, 6  $\times$  3 Ac, Val H $\beta$ ), 1.87–1.66 (6H, m, Lys H $\beta$ , H3f<sub>ax</sub>, H3f'<sub>ax</sub>), 1.66 (4H, m,  $J = 7.5$  Hz, Lys H $\delta$ ), 1.43–1.32 (4H, m, Lys H $\gamma$ ), 1.3 (3H, d,  $J = 7.5$  Hz, Ala H $\beta$ ), 1.13 (3H,  $J = 6.5$  Hz, Thr H $\gamma$ ), 0.89 (6H, d, 7.0 Hz, Val H $\gamma$ ). HSQC (<sup>1</sup>H, 500 MHz)/(<sup>13</sup>C, 126 MHz, deuterium oxide) 7.41/149.38 (H1g/C1g), 6.85/149.11 (H1g/C1g), 5.06/99.43 (H1c/C1c), 4.96/78.27 (H1a'/C1a'), 4.95/67.43 (H6f/C6f, H6f'/C6f'), 4.87/96.94 (H1c'/C1c'), 4.69/100.39 (H1b/C1b), 4.59/49.87 (H $\alpha$  Asn/C $\alpha$  Asn), 4.52/99.60 (H1a/C1a, H1d/C1d, H1d'/C1d'), 4.39/57.76 (H $\alpha$  Thr/C $\alpha$  Thr), 4.36/103.72 (H1e/C1e, H1e'/C1e'), 4.33/53.57 (H $\alpha$  Lys/C $\alpha$  Lys), 4.32/67.08 (H $\beta$  Thr/C $\beta$  Thr), 4.23/49.46 (H $\alpha$  Ala/C $\alpha$  Ala), 4.17/72.10 (H2b/C2b, H2g/C2g, H6f/C6f, H6f'/C6f'), 4.12/76.41 (H2c/C2c), 4.07/59.53 (H $\alpha$  Val/C $\alpha$  Val), 4.04/76.23 (H2c'/C2c'), 3.99/52.63 (H $\alpha$  Lys/C $\alpha$  Lys), 3.46/49.76 (H3 g/C3 g), 2.92/39.12 (He Lys/C $\epsilon$  Lys), 2.64/36.66 (H $\beta$  Asn/C $\beta$  Asn), 2.58/39.18 (H3f/C3f, H3f'/C3f'), 1.97/30.60 (H $\beta$  Val/C $\beta$  Val), 1.81/39.05 (H3f/C3f, H3f'/C3f'), 1.77/30.39 (H $\beta$  Lys/C $\beta$  Lys), 1.62/26.13 (H $\delta$  Lys/C $\delta$  Lys), 1.37/21.38 (H $\gamma$  Lys/C $\gamma$  Lys), 1.34/16.54 (H $\beta$  Ala/C $\beta$  Ala), 1.16/18.82 (H $\gamma$  Thr/C $\gamma$  Thr), 0.85/17.73 (H $\gamma$  Val/C $\gamma$  Val). HRMS, calculated for C<sub>112</sub>H<sub>185</sub>N<sub>23</sub>O<sub>66</sub> [M + 3H]<sup>3+</sup> 970.4020, found 970.3925. [M + 2H]<sup>2+</sup> 1455.0991, found 1455.0845.

**Azido amide oxime SGP (11c).** Yield 94.2%. <sup>1</sup>H NMR (500 MHz, deuterium oxide)  $\delta$  7.48 (1.6H, dd,  $J = 7.0$ , 3.7 Hz, H1g), 6.89 (0.4H, dd,  $J = 7.0$ , 2.5 Hz, H1g), 5.05 (1.4H, s, H1c, H6f, H6f'), 4.95 (1H, d,  $J = 9.7$  Hz, H1a'), 4.87 (1H, s, H1c'), 4.67 (1H, s, H1b), 4.60 (1H, t, Asn H $\alpha$ ), 4.52 (3H, d,  $J = 7.1$  Hz, H1a, H1d, H1d'), 4.49–4.41 (4H, m, H2g), 4.38 (1H, d, Thr H $\alpha$ ), 4.36 (2H, dd, H1e, H1e'), 4.33–4.29 (2H, m, Lys H $\alpha$ , Thr H $\beta$ ), 4.24 (1H, q,  $J = 7.2$  Hz, Ala H $\alpha$ ), 4.18 (2.6H, m, H1b, H6f, H6f'), 4.11 (1H, d,  $J = 2.5$  Hz, H2c), 4.06 (1H, d,  $J = 7.6$  Hz, Val H $\alpha$ ), 4.03 (1H, d,  $J = 2$  Hz, H2c'), 3.98 (1H, t,  $J = 6.7$  Hz, Lys H $\alpha$ ), 3.37–3.15 (8H, m, H4 g, H6 g), 2.91 (4H, q,  $J = 7.6$  Hz, Lys H $\epsilon$ ), 2.70 (2H, ddd,  $J = 62.2$ , 16.4, 6.7 Hz, Asn H $\beta$ ), 2.56 (2H, dd,  $J = 11.0$  Hz, H3f<sub>eq</sub>, H3f'<sub>eq</sub>), 1.80 (4H, m, Lys H $\beta$ ), 1.72 (6H, m, H5g, H3f<sub>ax</sub>, H3f'<sub>ax</sub>), 1.43–1.31 (4H, m, Lys H $\gamma$ ), 1.29 (3H, d, Ala H $\beta$ ), 1.11 (3H, d,  $J = 6.4$  Hz, Thr H $\gamma$ ), 0.88 (6H, d,  $J = 6.7$  Hz, Val H $\gamma$ ). HSQC (<sup>1</sup>H, 500 MHz)/(<sup>13</sup>C, 126 MHz, deuterium oxide) 7.49/150.77 (H1g/C1g), 6.90/150.47 (H1g/C1g), 5.06/99.43 (H1c/C1c), 5.05/67.26 (H6f/C6f, H6f'/C6f'), 4.96/78.16 (H1a'/C1a'), 4.88/97.00 (H1c'/C1c'), 4.70/100.37 (H1b/C1b), 4.60/49.86 (H $\alpha$  Asn/C $\alpha$  Asn), 4.53/99.51 (H1a/C1a, H1d/C1d, H1d'/C1d'), 4.48/72.14 (H2g/C2g), 4.39/57.99 (H $\alpha$  Thr/C $\alpha$  Thr), 4.37/103.58 (H1e/C1e, H1e'/C1e'), 4.33/53.62 (H $\alpha$  Lys/C $\alpha$  Lys), 4.32/67.14 (H $\beta$  Thr/C $\beta$  Thr), 4.24/49.53 (H $\alpha$  Ala/C $\alpha$  Ala), 4.18/72.35 (H2b/C2b, H6f/C6f, H6f'/C6f'), 4.12/76.11 (H2c/C2c), 4.08/59.56 (H $\alpha$  Val/C $\alpha$  Val), 4.04/76.01 (H2c'/C2c'), 4.00/52.70 (H $\alpha$  Lys/C $\alpha$  Lys), 3.32/36.54 (H4 g/C4 g), 3.31/48.73 (H6 g/C6 g), 3.23/36.58 (H4 g/C4 g), 2.93/39.11 (He Lys/C $\epsilon$  Lys), 2.77/36.47 (H $\beta$  Asn/C $\beta$  Asn), 2.58/39.32 (H3f/C3f, H3f'/C3f'), 2.04/29.84 (H $\beta$  Val/C $\beta$  Val), 1.87/30.45 (H $\beta$  Lys/C $\beta$  Lys), 1.78/39.39 (H3f/C3f, H3f'/C3f'), 1.71/27.53 (H5g/C5g), 1.63/26.18 (H $\delta$  Lys/C $\delta$  Lys), 1.37/21.65 (H $\gamma$  Lys/C $\gamma$  Lys), 1.34/16.85 (H $\beta$  Ala/C $\beta$  Ala), 1.09/18.70

(H $\gamma$  Thr/C $\gamma$  Thr), 0.86/17.86 (H $\gamma$  Val/C $\gamma$  Val). HRMS, calculated for C<sub>118</sub>H<sub>195</sub>N<sub>25</sub>O<sub>68</sub> [M + 3H]<sup>3+</sup> 1017.7601, found 1017.7606; [M + 2H]<sup>2+</sup> 1526.1363, found 1526.1346.

**Alkyne oxime SGP (11d).** Yield 88%. <sup>1</sup>H NMR (500 MHz, deuterium oxide)  $\delta$  7.49 (1.7H, dd,  $J = 7.0$ , 4.1 Hz, H1g), 6.90 (0.3H, dd,  $J = 7.0$ , 3.9 Hz, H1g), 5.07 (1.3H, s, H1c, H6f, H6f'), 4.96 (1H, d,  $J = 9.6$  Hz, H1a'), 4.88 (1H, s, H1c'), 4.67 (1H, s, H1b), 4.60 (1H, t,  $J = 6.5$  Hz, 1H, Asn H $\alpha$ ), 4.51 (7H, m, H1a, H1d, H1d', H2g), 4.40 (1H, d, Thr H $\alpha$ ), 4.38 (2H, dd, H1e, H1e'), 4.33–4.30 (2H, m, Lys H $\alpha$ , Thr H $\beta$ ), 4.24 (1H, q,  $J = 7.2$  Hz, Ala H $\alpha$ ), 4.18 (2.7H, m, H1b, H6f, H6f'), 4.12 (1H, d,  $J = 2.5$  Hz, H2c), 4.06 (1H, d,  $J = 7.6$  Hz, Val H $\alpha$ ), 4.03 (1H, d,  $J = 2$  Hz, H2c'), 3.98 (1H, t,  $J = 6.7$  Hz, Lys H $\alpha$ ), 2.92 (q,  $J = 7.5$  Hz, 4H, Lys H $\epsilon$ ), 2.81–2.61 (ddd,  $J = 62.3$ , 16.4, 6.7 Hz, 2H, Asn H $\beta$ ), 2.60–2.51 (3H, m, H3f<sub>eq</sub>, H3f'<sub>eq</sub>, H6 g), 2.05–1.87 (19H, m, Ac, Val H $\beta$ ), 1.87–1.66 (6H, m, Lys H $\beta$ , H3f<sub>ax</sub>, H3f'<sub>ax</sub>), 1.62 (4H, m,  $J = 7.5$  Hz, Lya H $\delta$ ), 1.38 (4H, d,  $J = 5.9$  Hz, Lys H $\gamma$ ), 1.30 (3H, d,  $J = 7.2$  Hz, Ala H $\beta$ ), 1.12 (3H, d,  $J = 6.4$  Hz, Thr H $\gamma$ ), 0.89 (6H, d,  $J = 6.7$  Hz, Val H $\gamma$ ). HSQC (<sup>1</sup>H, 500 MHz)/(<sup>13</sup>C, 126 MHz, deuterium oxide) 7.49/150.71 (H1g/C1g), 6.90/150.28 (H1g/C1g), 5.06/99.53 (H1c/C1c), 5.03/67.24 (H6f/C6f, H6f'/C6f'), 4.96/78.25 (H1a'/C1a'), 4.88/96.92 (H1c'/C1c'), 4.70/100.20 (H1b/C1b), 4.60/49.87 (H $\alpha$  Asn/C $\alpha$  Asn), 4.53/99.93 (H1a/C1a, H1d/C1d, H1d'/C1d'), 4.51/72.14 (H2g/C2g), 4.39/58.01 (H $\alpha$  Thr/C $\alpha$  Thr), 4.37/103.63 (H1e/C1e, H1e'/C1e'), 4.33/53.61 (H $\alpha$  Lys/C $\alpha$  Lys), 4.32/67.03 (H $\beta$  Thr/C $\beta$  Thr), 4.24/49.50 (H $\alpha$  Ala/C $\alpha$  Ala), 4.18/72.67 (H2b/C2b, H6f/C6f, H6f'/C6f'), 4.12/76.11 (H2c/C2c), 4.08/59.45 (H $\alpha$  Val/C $\alpha$  Val), 4.04/76.17 (H2c'/C2c'), 3.99/52.61 (H $\alpha$  Lys/C $\alpha$  Lys), 3.98/28.50 (H4 g/C4 g), 2.92/38.96 (He Lys/C $\epsilon$  Lys), 2.76/36.56 (H $\beta$  Asn/C $\beta$  Asn), 2.58/39.41 (H3f/C3f, H3f'/C3f'), 2.56/72.13 (H6 g/C6 g), 2.03/30.15 (H $\beta$  Val/C $\beta$  Val), 1.86/30.31 (H $\beta$  Lys/C $\beta$  Lys), 1.79/39.19 (H3f/C3f, H3f'/C3f'), 1.62/26.04 (H $\delta$  Lys/C $\delta$  Lys), 1.37/21.44 (H $\gamma$  Lys/C $\gamma$  Lys), 1.34/16.69 (H $\beta$  Ala/C $\beta$  Ala), 1.16/18.82 (H $\gamma$  Thr/C $\gamma$  Thr), 0.92/17.91 (H $\gamma$  Val/C $\gamma$  Val). HRMS, calculated for C<sub>118</sub>H<sub>189</sub>N<sub>19</sub>O<sub>68</sub> [M + 3H]<sup>3+</sup> 987.7383, found 987.7380; [M + 2H]<sup>2+</sup> 1481.1036, found 1481.1070.

**Alkyne amide oxime SGP (11e).** Yield 86.6%. <sup>1</sup>H NMR (500 MHz, deuterium oxide)  $\delta$  7.39 (1.6H, dd,  $J = 7.2$ , 3.3 Hz, H1 of oxime), 6.85 (0.4H, dd,  $J = 6.7$ , 2.6 Hz, H1 of oxime), 5.07 (1H, s, H1c), 4.96 (1.4H, d,  $J = 9.6$  Hz, H1a', H6f/f'), 4.88 (1H, s, H1c'), 4.76 (1H, s, H1b), 4.61 (5H, m, H2g, Asn H $\alpha$ ), 4.54 (3H, d,  $J = 6.7$  Hz, H1a, H1d, H1d'), 4.39 (1H, d,  $J = 3.5$  Hz, Thr H $\alpha$ ), 4.37 (1H, d,  $J = 2.5$  Hz, H1e), 4.35 (1H, d,  $J = 3$  Hz, H1e'), 4.34–4.28 (2H, m, Lys1 H $\alpha$ , Thr H $\beta$ ), 4.24 (1H, q,  $J = 7$  Hz, Ala H $\alpha$ ), 4.18 (1H, s, H2b), 4.16 (1.6H, dd,  $J = 10.0$  Hz, 7.5 Hz, H6f/f'), 4.12 (1H, d,  $J = 2$  Hz, H2c), 4.08 (1H, d,  $J = 8$  Hz, Val H $\alpha$ ), 4.04 (1H, d,  $J = 2$  Hz, H2c') 3.99 (1H, t,  $J = 6.5$  Hz, Lys2 H $\alpha$ ), 2.92 (4H, q,  $J = 7.5$  Hz, Lys H $\epsilon$ ), 2.86 (2H, q, H3 g), 2.81–2.61 (2H, m, Asn H $\beta$ ), 2.61–2.51 (2H, dd,  $J = 12.5$  Hz, 2.5 Hz, H3f<sub>eq</sub>, H3f'<sub>eq</sub>), 2.03–1.88 (19H, m, 6  $\times$  3 Ac, Val H $\beta$ ), 1.87–1.66 (6H, m, Lys H $\beta$ , H3f<sub>ax</sub>, H3f'<sub>ax</sub>), 1.66 (4H, m,  $J = 7.5$  Hz, Lya H $\delta$ ), 1.43–1.32 (4H, m, Lys H $\gamma$ ), 1.3 (3H, d,  $J = 7.5$  Hz, Ala H $\beta$ ), 1.13 (3H,  $J = 6.5$  Hz, Thr H $\gamma$ ), 0.89 (6H, d, 7.0 Hz, Val H $\gamma$ ). HSQC (<sup>1</sup>H, 500 MHz)/(<sup>13</sup>C, 126 MHz, deuterium oxide) 7.41/150.05 (H1g/C1g), 6.88/149.59

(H1g/C1g), 5.09/99.34 (H1c/C1c), 4.98/78.34 (H1a'/C1a'), 4.97/67.43 (H6f/C6f, H6f'/C6f'), 4.91/96.89 (H1c'/C1c'), 4.72/100.33 (H1b/C1b), 4.63/61.46 (H2g/C2g), 4.62/49.85 (H $\alpha$  Asn/C $\alpha$  Asn), 4.55/99.74 (H1a/C1a, H1d/C1d, H1d'/C1d'), 4.42/58.25 (H $\alpha$  Thr/C $\alpha$  Thr), 4.39/103.91 (H1e/C1e, H1e'/C1e'), 4.35/53.53 (H $\alpha$  Lys/C $\alpha$  Lys), 4.34/67.11 (H $\beta$  Thr/C $\beta$  Thr), 4.26/49.43 (H $\alpha$  Ala/C $\alpha$  Ala), 4.20/70.52 (H2b/C2b, H6f/C6f, H6f'/C6f'), 4.14/76.54 (H2c/C2c), 4.10/59.64 (H $\alpha$  Val/C $\alpha$  Val), 4.06/76.25 (H2c'/C2c'), 4.02/52.83 (H $\alpha$  Lys/C $\alpha$  Lys), 2.94/39.16 (H $\epsilon$  Lys/C $\epsilon$  Lys), 2.89/76.16 (H4 g/C4 g), 2.78/37.03 (H $\beta$  Asn/C $\beta$  Asn), 2.58/39.45 (H3f/C3f, H3f'/C3f'), 2.01/30.19 (H $\beta$  Val/C $\beta$  Val), 1.84/30.59 (H $\beta$  Lys/C $\beta$  Lys), 1.79/39.37 (H3f/C3f, H3f'/C3f'), 1.65/26.40 (H $\delta$  Lys/C $\delta$  Lys), 1.43/21.61 (H $\gamma$  Lys/C $\gamma$  Lys), 1.32/16.78 (H $\beta$  Ala/C $\beta$  Ala), 1.14/19.15 (H $\gamma$  Thr/C $\gamma$  Thr), 0.91/18.15 (H $\gamma$  Val/C $\gamma$  Val). HRMS, calculated for C<sub>114</sub>H<sub>183</sub>N<sub>17</sub>O<sub>66</sub> [M + 3H]<sup>3+</sup> 949.7240, found 949.7164; [M + 2H]<sup>2+</sup> 1424.0821, found 1424.0687.

**Synthesis of non-natural amine-SGPs (11b and 11f).** 10 mg CHO-SGP **8** (3.65  $\mu$ mol, 1.0 eq.) was dissolved in methane/PB (50 mM, pH 6.25) 1 : 1 solution. Then, 3-azido-1-propanamine **9a** or propargylamine **9b** (30.0 eq.), NaCNBH<sub>3</sub> (4.6 mg, 73  $\mu$ mol, 20.0 eq.) was added to the mixture in an ice bath. After 3 hours when RP-HPLC (Method B) indicated the completion of the reaction, the mixture was subjected to semi-preparative HPLC purification (Method D). The fractions containing the products was combined and lyophilized to obtain **11b** and **11f** as a white powder.

**Azido amine SGP (11b).** (9.0 mg, yield 84.8%). <sup>1</sup>H NMR (500 MHz, deuterium oxide)  $\delta$  5.03 (1H, s, H1c), 4.93 (1H, d,  $J$  = 9.6 Hz, H1a'), 4.83 (1H, s, H1c'), 4.70 (1H, s, H1b), 4.56 (1H, t,  $J$  = 6.7 Hz, Asn H $\alpha$ ), 4.50 (3H, dd,  $J$  = 6.4, 5.1 Hz, H1a, H1d, H1d'), 4.37 (1H, d,  $J$  = 3.5 Hz, Thr H $\alpha$ ), 4.35 (1H, d,  $J$  = 2.5 Hz, H1e), 4.34 (1H, d,  $J$  = 3 Hz, H1e'), 4.30 (2H, m, Lys1 H $\alpha$ , Thr H $\beta$ ), 4.21 (1H, q,  $J$  = 7.2 Hz, Ala H $\alpha$ ), 4.14 (1H, s, H2b), 4.09 (1H, d,  $J$  = 2.7 Hz, H2c), 4.05 (1H, d,  $J$  = 7.6 Hz, Val H $\alpha$ ), 4.01 (1H, d,  $J$  = 3.5 Hz, H2c'), 4.00–3.90 (3H, m, Lys H $\alpha$ , H6f, H6f'), 3.24–3.04 (8H, m,  $-2 \times -\text{CH}_2-\text{NH}-\text{CH}_2-$ ), 2.92 (4H, q,  $J$  = 7.5 Hz, Lys H $\epsilon$ ), 2.81–2.61 (2H, m, Asn H $\beta$ ), 2.61–2.51 (2H, dd,  $J$  = 12.5 Hz, 2.5 Hz, H3f<sub>eq</sub>, H3f'<sub>eq</sub>), 2.03–1.90 (19H, m, 6  $\times$  3 Ac, Val H $\beta$ ), 1.90–1.84 (4H, m, H3 g), 1.84–1.65 (6H, m, Lys H $\beta$ , H3f<sub>ax</sub>, H3f'<sub>ax</sub>), 1.59 (4H, m,  $J$  = 7.5 Hz, Lys H $\delta$ ), 1.40–1.29 (4H, m, Lys H $\gamma$ ), 1.27 (3H, d,  $J$  = 7.5 Hz, Ala H $\beta$ ), 1.10 (3H,  $J$  = 6.5 Hz, Thr H $\gamma$ ), 0.86 (6H, d, 7.0 Hz, Val H $\gamma$ ). HSQC ((<sup>1</sup>H, 500 MHz)/(<sup>13</sup>C, 126 MHz), deuterium oxide) 5.05/99.53 (H1c/C1c), 4.96/78.22 (H1a'/C1a'), 4.85/96.87 (H1c'/C1c'), 4.69/100.38 (H1b/C1b), 4.59/49.84 (H $\alpha$  Asn/C $\alpha$  Asn), 4.53/99.58 (H1a/C1a, H1d/C1d, H1d'/C1d'), 4.38/58.04 (H $\alpha$  Thr/C $\alpha$  Thr), 4.37/103.51 (H1e/C1e, H1e'/C1e'), 4.32/53.51 (H $\alpha$  Lys/C $\alpha$  Lys), 4.31/67.02 (H $\beta$  Thr/C $\beta$  Thr), 4.23/49.46 (H $\alpha$  Ala/C $\alpha$  Ala), 4.17/70.16 (H2b/C2b), 4.11/76.42 (H2c/C2c), 4.07/59.39 (H $\alpha$  Val/C $\alpha$  Val), 4.03/76.11 (H2c'/C2c'), 3.99/52.73 (H $\alpha$  Lys/C $\alpha$  Lys), 3.43/48.19 (H4g/C4g), 3.21/48.59 (H2g/C2g), 3.16/46.14 (H1g/C1g), 2.91/39.01 (H $\epsilon$  Lys/C $\epsilon$  Lys), 2.76/36.86 (H $\beta$  Asn/C $\beta$  Asn), 2.59/39.43 (H3f/C3f, H3f'/C3f'), 1.98/30.12 (H $\beta$  Val/C $\beta$  Val), 1.80/30.30 (H $\beta$  Lys/C $\beta$  Lys), 1.75/39.63 (H3f/C3f, H3f'/C3f'), 1.59/26.28 (H $\delta$  Lys/C $\delta$  Lys), 1.36/21.42 (H $\gamma$  Lys/C $\gamma$  Lys), 1.29/16.67 (H $\beta$  Ala/C $\beta$  Ala), 1.12/19.03 (H $\gamma$  Thr/C $\gamma$  Thr), 0.88/18.21

(H $\gamma$  Val/C $\gamma$  Val). HRMS, calculated for C<sub>114</sub>H<sub>193</sub>N<sub>23</sub>O<sub>64</sub> [M + 4H]<sup>4+</sup> 728.0717, found 728.0717; [M + 3H]<sup>3+</sup> 970.4263, found 970.4254; [M + 2H]<sup>2+</sup> 1455.1356, found 1455.1381.

**Alkyne amine SGP (11f).** (8.5 mg, 3.0  $\mu$ mol, yield 82.2%). <sup>1</sup>H NMR (500 MHz, deuterium oxide)  $\delta$  5.15 (1H, s, H1c), 5.05 (1H, d,  $J$  = 9.6 Hz, H1a'), 4.95 (1H, s, H1c'), 4.84 (1H, s, H1b), 4.67 (1H, t,  $J$  = 6.7 Hz, Asn H $\alpha$ ), 4.62 (3H, dd,  $J$  = 6.4, 5.1 Hz, H1a, H1d, H1d'), 4.46 (2H, dd,  $J$  = 7 Hz, H1e, H1e'), 4.41 (1H, t, Lys1 H $\alpha$ ), 4.31 (1H, q,  $J$  = 7.2 Hz, Ala H $\alpha$ ), 4.26 (1H, s, H2b), 4.22 (1H, m, Thr H $\beta$ ) 4.21 (1H, m, Thr H $\alpha$ ), 4.17–4.10 (3H, m, H2c, Val H $\alpha$ , H2c'), 4.01 (4H, H2g), 3.43–3.16 (4H, m, H1g), 3.01 (6H, m, Lys H $\epsilon$ , H4g), 2.93–2.69 (2H, m, Asn H $\beta$ ), 2.69–2.59 (2H, dd,  $J$  = 12.5 Hz, 2.5 Hz, H3f<sub>eq</sub>, H3f'<sub>eq</sub>), 2.15ii–1.90 (16iH, m, 5  $\times$  3 Ac, Val H $\beta$ ), 1.97–1.81 (7H, m, Lys H $\beta$ , Ac) 1.80–1.64 (6H, m, Lys H $\beta$ , H3f<sub>ax</sub>, H3f'<sub>ax</sub>), 1.66 (4H, m,  $J$  = 7.5 Hz, Lys H $\delta$ ), 1.43–1.32 (4H, m, Lys H $\gamma$ ), 1.3 (3H, d,  $J$  = 7.5 Hz, Ala H $\beta$ ), 1.13 (3H,  $J$  = 6.5 Hz, Thr H $\gamma$ ), 0.89 (6H, d, 7.0 Hz, Val H $\gamma$ ). HSQC ((<sup>1</sup>H, 500 MHz)/(<sup>13</sup>C, 126 MHz), deuterium oxide) 5.06/100.47 (H1c/C1c), 4.96/79.04 (H1a'/C1a'), 4.86/97.82 (H1c'/C1c'), 4.70/101.42 (H1b/C1b), 4.59/50.87 (H $\alpha$  Asn/C $\alpha$  Asn), 4.53/100.62 (H1a/C1a, H1d/C1d, H1d'/C1d'), 4.37/103.51 (H1e/C1e, H1e'/C1e'), 4.32/54.42 (H $\alpha$  Lys/C $\alpha$  Lys), 4.31/67.02 (H $\beta$  Thr/C $\beta$  Thr), 4.22/50.36 (H $\alpha$  Ala/C $\alpha$  Ala), 4.17/71.01 (H2b/C2b), 4.12/77.38 (H2c/C2c), 4.06/60.90 (H $\alpha$  Val/C $\alpha$  Val), 4.04/77.09 (H2c'/C2c'), 3.92/53.74 (H $\alpha$  Lys/C $\alpha$  Lys), 3.91/37.48 (H2g/C2g), 3.28/48.52 (H1g/C1g), 2.90/39.89 (H $\epsilon$  Lys/C $\epsilon$  Lys), 2.79/39.26 (H $\beta$  Asn/C $\beta$  Asn), 2.60/40.92 (H3f/C3f, H3f'/C3f'), 1.97/30.09 (H $\beta$  Val/C $\beta$  Val), 1.79/31.46 (H $\beta$  Lys/C $\beta$  Lys), 1.69/41.18 (H3f/C3f, H3f'/C3f'), 1.65/27.10 (H $\delta$  Lys/C $\delta$  Lys), 1.35/22.40 (H $\gamma$  Lys/C $\gamma$  Lys), 1.30/17.64 (H $\beta$  Ala/C $\beta$  Ala), 1.09/20.15 (H $\gamma$  Thr/C $\gamma$  Thr), 0.89/19.16 (H $\gamma$  Val/C $\gamma$  Val). HRMS, calculated for C<sub>114</sub>H<sub>187</sub>N<sub>17</sub>O<sub>64</sub> [M + 4H]<sup>4+</sup> 705.5554, found 705.5570; [M + 3H]<sup>3+</sup> 940.4045, found 940.4066; [M + 2H]<sup>2+</sup> 1410.1029, found 1410.1140.

**Synthesis of azido oxime sialoglycan 12.** Azido oxime SGP **11a** (8.7 mg, 3.0  $\mu$ mol) was incubated with *endo*-M (43.5  $\mu$ g) in PB (50 mM pH 6.5, 87  $\mu$ L) at 30 °C and monitored by HPLC. The residue was subjected to semi-preparative HPLC purification to give the pure azido oxime sialo glycan **12** as a white powder (5.5 mg, yield 88.87%). <sup>1</sup>H NMR (500 MHz, deuterium oxide)  $\delta$  7.39 (dd,  $J$  = 7.2, 4.8 Hz, 1.3H,  $-\text{N}=\text{CH}-$ ), 6.83 (dd,  $J$  = 6.6, 4.0 Hz, 0.7H,  $-\text{N}=\text{CH}-$ ), 5.11 (d,  $J$  = 3.1 Hz, 0.8H, H1a( $\alpha$ )), 5.05 (s, 1H, H1c), 4.94 (dd,  $J$  = 9.0, 6.6 Hz, 0.7H, H6f/f'), 4.86 (s, 1H, H1c'), 4.50 (d,  $J$  = 7.3 Hz, 2H, H1d/d'), 4.33 (d,  $J$  = 7.9 Hz, 2H, H1e/e'), 4.22–4.12 (m, 6.3H, H2b,  $-\text{CH}_2-\text{O}-\text{N}=\text{C}$ , H6f/f'), 4.09 (s, 1H, H2c), 4.02 (s, 1H, H2c'), 3.92–3.76 (m, 14H, H2a, H6'b, H3c, H3c', H6'c, H6'c', H6d, H6d', H6'd, H6'd', H4e, H4e', H6'e, H6'e'), 3.68 (m, 20H), 3.58–3.38 (m, 21H), 1.99–1.87 (m, 15H), 2.55 (d,  $J$  = 11.8 Hz, 2H, H3f<sub>eq</sub>/f'<sub>eq</sub>), 2.00–1.85 (m, 15H, Ac), 1.77 (t,  $J$  = 11.4 Hz, 2H, H3f<sub>ax</sub>/f'<sub>ax</sub>). HSQC ((<sup>1</sup>H, 500 MHz)/(<sup>13</sup>C, 126 MHz), deuterium oxide) 7.39/149.30 (H1g/C1g), 6.83/149.30 (H1g/C1g), 5.11/90.40 (H1a $\alpha$ /C1a $\alpha$ ), 5.05/99.56 (H1c/C1c), 4.95/67.23 (H6f/C6f, H6f'/C6f'), 4.86/96.91 (H1c'/C1c'), 4.68/100.36 (H1b/C1b), 4.62/94.73 (H1a $\beta$ /C1a $\beta$ ), 4.50/99.20 (H1d/C1d, H1d'/C1d'), 4.34/103.64 (H1e/C1e, H1e'/C1e'), 4.16/72.65 (H2b/C2b, H2g/C2g, H6f/C6f, H6f'/C6f'),

4.10/76.23 (H2c/C2c), 4.03/76.06 (H2c'/C2c'), 3.44/49.89 (H3 g/C3 g), 2.54/39.18 (H3f/C3f, H3f'/C3f'), 1.77/38.84 (H3f/C3f, H3f'/C3f'). HRMS, calculated for  $C_{76}H_{121}N_{13}O_{53}$   $[M + 2H]^{2+}$  1032.8664, found  $[M + 2H]^{2+}$  1032.8665,  $[M + 3H]^{3+}$  688.9136, found 688.9182.

**Synthesis of oxime sialoglycan oxazoline 13.** 5.0 mg (2.42  $\mu$ mol, 1.0 eq) **12**, 34.0  $\mu$ L ddH<sub>2</sub>O, 11.0 mg (108.9  $\mu$ mol, 15.0  $\mu$ L, 45.0 eq.) Et<sub>3</sub>N and 6.2 mg (36.3  $\mu$ mol, 15.0 eq.) DMC was added to a tube successively in an ice bath for 1 hour after which the proton NMR indicated the complete transformation of the starting material to the corresponding oxazoline with an azido functional group. The solution was desalted by using a Sephadex G-25 column, which was eluted with water containing 0.2% triethylamine. The product was combined and lyophilized to give **13** as a white powder (4.5 mg, 91%). <sup>1</sup>H NMR (500 MHz, deuterium oxide)  $\delta$  7.37 (d,  $J$  = 7.2 Hz, 1.6H, H1g), 6.80 (d,  $J$  = 6.6 Hz, 0.4H, H1g), 6.01 (d,  $J$  = 7.2 Hz, 1H, H1 of oxazoline), 5.11–4.96 (m, 1.4H, H1c, H6f, H6f'), 4.89 (s, 1H, H1c'), 4.66 (s, 1H, H1b), 4.53 (dd,  $J$  = 5.7 Hz, 2H, H1d, H1d'), 4.35 (d,  $J$  = 6.6 Hz, 2H, H1e, H1e'), 4.30 (s, 1H, H3a), 4.26–4.18 (dd,  $J$  = 9.7 Hz, 7.2 Hz, 1.6H, H6f, H6f'), 4.15 (t,  $J$  = 4.6 Hz, 4H, H2g), 4.11 (m, 1H, H2a), 4.09 (m, 1H, H2b), 2.55 (d,  $J$  = 13.2 Hz, 2H, H3f<sub>eq</sub>, H3f'<sub>eq</sub>), 2.13–1.83 (m, 15H, Ac), 1.67 (t, 2H, H3f<sub>ax</sub>, H3f'<sub>ax</sub>). HSQC (<sup>1</sup>H, 500 MHz)/(<sup>13</sup>C, 126 MHz, deuterium oxide) 7.39/150.81 (H1g/C1g), 6.82/150.84 (H1g/C1g), 6.02/100.66 (H1a/C1a oxa), 5.07/100.38 (H1c/C1c), 4.90/97.41 (H1c'/C1c'), 4.67/102.13 (H1b/C1b), 4.54/100.31 (H1d/C1d, H1d'/C1d'), 4.36/104.59 (H1e/C1e, H1e'/C1e'), 4.32/70.15 (H3a/C3a, oxa), 4.23/73.66 (H6f/C6f, H6f'/C6f'), 4.17/73.32 (H2g/C2g), 4.13/66.06 (H2a/C2a, oxa), 4.12/77.28 (H2c/C2c), 4.09/77.06 (H2c'/C2c'), 4.08/71.19 (H2b/C2b), 3.47/50.52 (H3 g/C3 g), 2.57/41.16 (H3f/C3f, H3f'/C3f'), 1.68/41.06 (H3f/C3f, H3f'/C3f'). ESI-HRMS, calculated for  $C_{76}H_{119}N_{13}O_{52}$   $[M + 2H]^{2+}$  1023.8612, found  $[M + 2H]^{2+}$  1023.8557,  $[M + H + Na]^{2+}$  1034.8521, found 1034.8508,  $[M + 2Na]^{2+}$  1045.8431, found 1045.8471.

**Synthesis of Herceptin-Fuc $\alpha$ 1,6GlcNAc (6).** A solution of commercial Herceptin (38 mg) in PB buffer (pH 7.5) was incubated with wild-type *endo*-S (150  $\mu$ g) at 37 °C for 2 hours. The SDS-PAGE analysis showed the complete deglycosylation of Herceptin. The antibody was loaded to protein A-agarose resin (3 mL), which was pre-washed with glycine-HCl (100 mM, pH 2.5, 25 mL) and pre-equilibrated with PB (50 mM, pH 8.0, 50 mL). The column was washed with PB (50 mM, pH 8.0) 50 mL and glycine-HCl (20 mM, pH 5.0, 30 mL) successively and the bound antibody was eluted with glycine-HCl (100 mM, pH 2.5) followed by neutralization to ~pH 7.5 with glycine-HCl (1 M, pH 8.8) immediately. The fractions containing the deglycosylated Herceptin **6** was combined and concentrated by centrifugal filtration through a 10 kDa cut-off membrane. And the concentration of the product was measured by using a Bicinchoninic Acid (BCA) Kit for protein determination following the manufacturer's protocol. LC-MS deconvolution data: calculated for Herceptin-Fuc $\alpha$ 1,6GlcNAc (**6**), 145806.06, found, 145805.35.

***endo*-S D233Q-catalyzed chemoenzymatic synthesis of glycoengineered Herceptins with **6** and purified oxazolines.** To

a solution of **6** (1 mg) in Tris buffer (50 mM, pH 7.4, 200  $\mu$ L) were added the purified oxazolines (**2–5**, **13**) (1.5 mM, 30 eq.) and *endo*-S D233Q (30  $\mu$ g). The reaction mixture was incubated at 30 °C for 1–2 hours. SDS-PAGE and LC-MS monitoring indicated the complete reaction. The reaction mixture was immediately subjected to affinity chromatography *via* protein A resin (100  $\mu$ L) following the above procedure to give the corresponding glycoengineered Herceptin **7a–d** and **14a**. LC-MS deconvolution data: calculated for S2G2F-Herceptin **7a** 149809.45, found 149810.52. Calculated for G2F-Herceptin **7b** 148645.06, found 148656.89. Calculated for G0F-Herceptin **7c** 147996.85, found 147997.27. Calculated for Man3GlcNAc2F-Herceptin **7d** 147184.54, found 147185.75. Calculated for azido-oxime-S2G2F-Herceptin **14a** 149897.47, found 149890.43 (see the ESI† for more details).

**One-pot chemoenzymatic synthesis of glycoengineered Herceptin with **6** and *in situ* oxazolines.** SGP (**1**) or SGP non-natural derivatives (**11a–e**, 10 mg) were incubated with *endo*-M (50  $\mu$ g) in PB (50 mM, pH 6.25, 50  $\mu$ L) at 30 °C. After 3–4 hours, RP-HPLC (Method B) monitoring indicated the complete hydrolysis of GlcNAc-peptide from the glycopeptide. Then the mixture was diluted to 50 mM with water, and DMC (15 eq.) and Et<sub>3</sub>N (40 eq.) was added. The solution was put on an ice bath for 1–2 hours. Then, the reaction mixture was further diluted into 2 mL Tris buffer (50 mM, pH 7.4) containing **6** (10 mg) and *endo*-S D233Q (300  $\mu$ g). The residue was incubated at 30 °C for 1–2 hours, monitored by SDS-PAGE and LC-MS. After affinity chromatography *via* protein A resin, glycoengineered Herceptin **7a** and **14a–e** were obtained. LC-MS deconvolution data: calculated for azido-oxime-S2G2F-Herceptin **14a** 149897.47, found 149909.91. Calculated for azido-amine-S2G2F-Herceptin **14b** 149897.62, found 149906.31. Calculated for azido-amide-oxime-S2G2F-Herceptin **14c** 150181.62, found 150191.82. Calculated for alkyne-amide-oxime-S2G2F-Herceptin **14d** 150001.49, found 150002.00. Calculated for alkyne-oxime-S2G2F-Herceptin **14e** 149773.41, found 149772.38. (see the ESI† for more details).

**Synthesis of glycosite-specific ADCs **22a–e**.** The azido Herceptin **14a** or **14b** (10 mg) was incubated with **21a–c** (130  $\mu$ M, 20 eq.) in PB (50 mM, pH 7.5, 10 mL) containing 10% DMSO at 30 °C for 4 h and monitored by SDS-PAGE and LC-MS. After the conjugation, the reaction mixture was subjected to affinity chromatography *via* protein A resin following the above procedure. Fractions containing the products were combined to give **22a–e**. LC-MS deconvolution data: **22a**, 154847.29; **22b**, 155684.74; **22c**, 156659.32; **22d**, 155688.26; **22e**, 156643.96.

**Synthesis of ADC **23**.** A solution of azido tagged Herceptin **14a** (1.0 mg mL<sup>-1</sup> 5 mg, 1.0 eq.) and DM1-SMCC (**20**) (100  $\mu$ M, 15.0 eq.) in a PB (50 mM, pH 7.5) containing 10% DMSO was incubated at 37 °C for 1 hour. LC-MS indicated the DAR of 2.6. The mixture was immediately subjected to affinity chromatography *via* a protein A resin column to give ADC **23**. LC-MS deconvolution data: 149907.63 (+0 DM1), 147719.04 (+1 DM1), 151823.00 (+2 DM1), 152786.70 (+3 DM1), 153734.55 (+4 DM1), 154696.10 (+5 DM1).

**Synthesis of dual-drug ADC 24.** A mixture of **23** ( $0.5 \text{ mg mL}^{-1}$ , 2 mg, 1.0 eq.) and DBCO-PEG<sub>4</sub>-VC-PAB-MMAE (**21c**,  $66.67 \text{ } \mu\text{M}$ , 20.0 eq.) was incubated at 30 °C. The SDS-PAGE and ESI-LCMS indicated complete conjugation. The solution was subjected to protein A resin purification to give the dual-drug ADC **24**. LCMS deconvolution data: 157606.71 (+1 DM1), 158566.82 (+2 DM1), 159530.22 (+3 DM1), 160477.23 (+4 DM1), 161446.46 (+5 DM1).

**Synthesis of glycosite-specific Cy5-labeled Herceptin 22f.** The azido tagged Herceptin **14a** ( $0.5 \text{ mg mL}^{-1}$ , 1 mg) was incubated with DBCO-Cy5 (**21d**, 61  $\mu\text{g}$ , 10.0 eq.) in PB (50 mM, pH 7.5) at 30 °C and monitored by SDS-PAGE or LCMS. The reaction buffer was subjected to protein A column purification to give the Cy5 labeled Herceptin **22f**. LC-MS deconvolution data: 153572.33.

**Synthesis of Cy5-labeled ADC 25.** ADC **23** ( $0.5 \text{ mg mL}^{-1}$ , 1 mg) was incubated with DBCO-Cy5 **21d** (61  $\mu\text{g}$ , 10.0 eq.) at 30 °C and monitored by SDS-PAGE or LCMS. The reaction buffer was subjected to protein A column purification to give the Cy5 labeled ADC **25**. LC-MS deconvolution data: 153561.22 (+0 DM1), 154520.53 (+1 DM1), 155476.70 (+2 DM1), 156431.15 (+3 DM1), 157393.21 (+4 DM1), 158349.16 (+5 DM1), 159310.31 (+6 DM1).

**PNGase-F digestion analysis of 14a and ADC 22c.** The site-specific transglycosylation and conjugation of **14a** and **22c** were analyzed after PNGase-F deglycosylation. Azido-tagged Herceptin **14a** ( $5.0 \text{ mg mL}^{-1}$ , 100  $\mu\text{g}$ ) was incubated with PNGaseF ( $0.1 \text{ mg mL}^{-1}$ ) overnight at 37 °C to give Herceptin-Asp<sup>297</sup> and released glycan **28**. SDS-PAGE indicated that an unnatural glycan was released from the antibody. The reaction solution was subjected to LC-MS analysis. Herceptin-Asp<sup>297</sup>, LC-MS deconvolution data: calculated 145109.75, found 145107.65. Released glycan **28**, HRMS: calculated for C<sub>90</sub>H<sub>144</sub>N<sub>14</sub>O<sub>62</sub> [M + 3H]<sup>3+</sup> 805.2927, found 805.2936; [M + 2H]<sup>2+</sup> 1207.4351, found 1207.4365. With a similar procedure, ADC **22c** was incubated with PNGase-F overnight at 37 °C to give deglycosylated Herceptin-Asp<sup>297</sup> and released glycan-drug complex **29**. SDS-PAGE and LCMS indicated that the unnatural glycan attached with MMAE was released from the antibody. The released glycan-drug complex **29**, HRMS: calculated for C<sub>270</sub>H<sub>408</sub>N<sub>38</sub>O<sub>100</sub> [M + 7H]<sup>7+</sup> 827.1222, found 827.1241; [M + 6H]<sup>6+</sup> 964.8080, found 964.9725. [M + 5H]<sup>5+</sup> 1157.5680, found 1157.5654; [M + 4H]<sup>4+</sup> 1446.7080, found 1446.6993. [M + 3H]<sup>3+</sup> 1928.6081, found 1928.6228.

**SK-BR-3 cell-based ELISA assay.** SK-BR-3 cells were cultured in a 96-well plate ( $1 \times 10^5$  cells per well) for 16 h at 37 °C. Cells were washed twice with PBS, and fixed with 4% paraformaldehyde/PBS buffer (pH 7.4). Commercial Herceptin, random labeled Cy5-Herceptin (**26**) and glycosite-specific labeled Cy5-Herceptin (**22f**) in 1% BSA/PBS were added to the wells and incubated for 30 min at 4 °C. Unbound proteins were removed and washed twice with 0.05% Tween 20/PBS (pH 7.4). Subsequently, the cells were blocked with 1% BSA/PBS at room temperature for 30 min, and then incubated with rabbit anti-human IgG1 Fc mAb (Sigma) for 60 min at 4 °C. After washing

twice, HRP-labeled goat anti-rabbit IgG (H + L) Ab (Yeason) was added to the wells, and left at 4 °C for 30 min. After adequate washing, 50 mL tetramethylbenzidine (TMB) reagent was added as the substrate for HRP, and the reaction was stopped with 2N H<sub>2</sub>SO<sub>4</sub>. Finally, absorbance was measured at 450 nm. The binding curves were analyzed by GraphPad software.

**Fluorescence cell imaging.** SK-BR-3 cells were cultured directly on slides with a Chamber Slide System (Nunc) for 16 h at 37 °C. Cells were washed twice with PBS and blocked using 1% BSA/PBS at room temperature for 30 min. 20  $\mu\text{g mL}^{-1}$  of Cy5-Herceptin **22f** was added to the wells and incubated for 30 min at 4 °C. After washing with 0.05% Tween 20/PBS (pH 7.4), the cells were fixed with 4% paraformaldehyde/4% sucrose/PBS solution at room temperature for 20 min. Hoechst (Sigma) staining was used for localization of nuclei at room temperature for 5 min. Extensive washing was done prior to confocal microscopy (Olympus) detection.

**Cell cytotoxicity.** The MTT (3-(4,5-dimethyl-2-thiazolyl)-2,5-diphenyl-2-H-tetrazolium bromide) method was used to measure the *in vitro* efficacy of the ADCs. SK-Br-3 cells were cultured in RPMI 1640 GlutaMAX (Invitrogen) supplemented with 10% fetal bovine serum (FBS) and were planted into 96-well plates with 8000 cells per well. These plates were incubated overnight at 37 °C and 5% CO<sub>2</sub>. The small molecules, DM1 and MMAE, were diluted 3 fold with the culture solution from an initial concentration of 100 nM to the final concentration of 0.41 nM. And ten-fold dilution was applied to the ADC samples from 10  $\mu\text{g mL}^{-1}$  to 0.0001  $\mu\text{g mL}^{-1}$ . The samples were added to three wells with every single concentration and the cells were cultured at 37 °C and 5% CO<sub>2</sub> for three days before the addition of MTT solution. 10% SDS solution was added to the cell culture solution which had been incubated with MTT for 4 h, to dissolve the formazan. Optical density (OD) was measured at 570 nm using an Epoch (BioTek) after incubation overnight at 37 °C and 5% CO<sub>2</sub>. Finally, the EC<sub>50</sub> values and the cell viability curve were calculated by GraphPad software.

## Acknowledgements

This work was supported by the National Natural Science Foundation of China (NNSFC, No. 21372238 and 21572244), the SIMM Institute Fund (CASIMM0120153004), and the "Personalized Medicines—Molecular Signature-based Drug Discovery and Development", Strategic Priority Research Program of the Chinese Academy of Sciences, Grant No. XDA12020311. We thank the mass spectrometry facility of the iHuman Institute for providing us the LC-MS and HPAEC instruments. We thank Dr Raymond Stevens, Dr Zhijie Liu, Dr Houchao Tao, and other colleagues in iHuman for helpful discussion. W. H. thanks his former supervisor Dr Lai-Xi Wang at the University of Maryland for his kind mentoring.

## References

- 1 S. Aggarwal, What's fueling the biotech engine-2010 to 2011, *Nat. Biotechnol.*, 2011, **29**(12), 1083–1089.
- 2 G. J. Weiner, Building better monoclonal antibody-based therapeutics, *Nat. Rev. Cancer*, 2015, **15**(6), 361–370.
- 3 S. Salemi, M. Markovic, G. Martini and R. D'Amelio, The expanding role of therapeutic antibodies, *Int. Rev. Immunol.*, 2015, **34**(3), 202–264.
- 4 A. Zumla, M. Rao, R. S. Wallis, S. H. Kaufmann, R. Rustomjee, P. Mwaba, C. Vilaplana, D. Yeboah-Manu, J. Chakaya, G. Ippolito, E. Azhar, M. Hoelscher and M. Maeurer, Host-directed therapies for infectious diseases: current status, recent progress, and future prospects, *Lancet Infect. Dis.*, 2016, **16**(4), e47–e63.
- 5 P. Sondermann and D. E. Szymkowski, Harnessing Fc receptor biology in the design of therapeutic antibodies, *Curr. Opin. Immunol.*, 2016, **40**, 78–87.
- 6 D. J. DiLillo and J. V. Ravetch, Fc-Receptor Interactions Regulate Both Cytotoxic and Immunomodulatory Therapeutic Antibody Effector Functions, *Cancer Immunol. Res.*, 2015, **3**(7), 704–713.
- 7 A. M. Brandsma, S. R. Jacobino, S. Meyer, T. Ten Broeke and J. H. Leusen, Fc receptor inside-out signaling and possible impact on antibody therapy, *Immunol. Rev.*, 2015, **268**(1), 74–87.
- 8 L. T. Vogelpoel, D. L. Baeten, E. C. De Jong and J. Den Dunnen, Control of cytokine production by human fc gamma receptors: implications for pathogen defense and autoimmunity, *Front. Immunol.*, 2015, **6**, 79.
- 9 A. Pincetic, S. Bournazos, D. J. DiLillo, J. Maamary, T. T. Wang, R. Dahan, B. M. Fiebiger and J. V. Ravetch, Type I and type II Fc receptors regulate innate and adaptive immunity, *Nat. Immunol.*, 2014, **15**(8), 707–716.
- 10 T. S. Raju, Terminal sugars of Fc glycans influence antibody effector functions of IgGs, *Curr. Opin. Immunol.*, 2008, **20**(4), 471–478.
- 11 R. M. Anthony and F. Nimmerjahn, The role of differential IgG glycosylation in the interaction of antibodies with FcγR3 in vivo, *Curr. Opin. Organ Transplant.*, 2011, **16**(1), 7–14.
- 12 C. Ferrara, S. Grau, C. Jager, P. Sondermann, P. Brunker, I. Waldhauer, M. Hennig, A. Ruf, A. C. Rufer, M. Stihle, P. Umana and J. Benz, Unique carbohydrate-carbohydrate interactions are required for high affinity binding between FcγR3 and antibodies lacking core fucose, *Proc. Natl. Acad. Sci. U. S. A.*, 2011, **108**(31), 12669–12674.
- 13 T. Shinkawa, K. Nakamura, N. Yamane, E. Shoji-Hosaka, Y. Kanda, M. Sakurada, K. Uchida, H. Anazawa, M. Satoh, M. Yamasaki, N. Hanai and K. Shitara, The absence of fucose but not the presence of galactose or bisecting N-acetylglucosamine of human IgG1 complex-type oligosaccharides shows the critical role of enhancing antibody-dependent cellular cytotoxicity, *J. Biol. Chem.*, 2003, **278**(5), 3466–3473.
- 14 R. M. Anthony, F. Wermeling and J. V. Ravetch, Novel roles for the IgG Fc glycan, *Ann. N. Y. Acad. Sci.*, 2012, **1253**, 170–180.
- 15 R. L. Shields, J. Lai, R. Keck, L. Y. O'Connell, K. Hong, Y. G. Meng, S. H. Weikert and L. G. Presta, Lack of fucose on human IgG1 N-linked oligosaccharide improves binding to human FcγR3 and antibody-dependent cellular toxicity, *J. Biol. Chem.*, 2002, **277**(30), 26733–26740.
- 16 W. Huang, J. Giddens, S. Q. Fan, C. Toonstra and L. X. Wang, Chemoenzymatic glycoengineering of intact IgG antibodies for gain of functions, *J. Am. Chem. Soc.*, 2012, **134**(29), 12308–12318.
- 17 M. J. Gramer, J. J. Eckblad, R. Donahue, J. Brown, C. Shultz, K. Vickerman, P. Priem, E. T. Van den Bremer, J. Gerritsen and P. H. Van Berkel, Modulation of antibody galactosylation through feeding of uridine, manganese chloride, and galactose, *Biotechnol. Bioeng.*, 2011, **108**(7), 1591–1602.
- 18 R. M. Anthony, F. Nimmerjahn, D. J. Ashline, V. N. Reinhold, J. C. Paulson and J. V. Ravetch, Recapitulation of IVIG anti-inflammatory activity with a recombinant IgG Fc, *Science*, 2008, **320**(5874), 373–376.
- 19 R. M. Anthony, F. Wermeling, M. C. Karlsson and J. V. Ravetch, Identification of a receptor required for the anti-inflammatory activity of IVIG, *Proc. Natl. Acad. Sci. U. S. A.*, 2008, **105**(50), 19571–19578.
- 20 Y. Kaneko, F. Nimmerjahn and J. V. Ravetch, Anti-inflammatory activity of immunoglobulin G resulting from Fc sialylation, *Science*, 2006, **313**(5787), 670–673.
- 21 A. Beck and J. M. Reichert, Marketing approval of mogamulizumab: a triumph for glyco-engineering, *mAbs*, 2012, **4**(4), 419–425.
- 22 A. M. Goetze, Y. D. Liu, Z. Zhang, B. Shah, E. Lee, P. V. Bondarenko and G. C. Flynn, High-mannose glycans on the Fc region of therapeutic IgG antibodies increase serum clearance in humans, *Glycobiology*, 2011, **21**(7), 949–959.
- 23 L. Alessandri, D. Ouellette, A. Acquah, M. Rieser, D. Leblond, M. Saltarelli, C. Radziejewski, T. Fujimori and I. Correia, Increased serum clearance of oligomannose species present on a human IgG1 molecule, *mAbs*, 2012, **4**(4), 509–520.
- 24 L. Liu, Antibody glycosylation and its impact on the pharmacokinetics and pharmacodynamics of monoclonal antibodies and Fc-fusion proteins, *J. Pharm. Sci.*, 2015, **104**(6), 1866–1884.
- 25 A. Beck, O. Cochet and T. Wurch, GlycoFi's technology to control the glycosylation of recombinant therapeutic proteins, *Expert Opin. Drug Discovery*, 2010, **5**(1), 95–111.
- 26 H. Li, N. Sethuraman, T. A. Stadheim, D. Zha, B. Prinz, N. Ballew, P. Bobrowicz, B. K. Choi, W. J. Cook, M. Cukan, N. R. Houston-Cummings, R. Davidson, B. Gong, S. R. Hamilton, J. P. Hoopes, Y. Jiang, N. Kim, R. Mansfield, J. H. Nett, S. Rios, R. Strawbridge, S. Wildt and T. U. Gerngross, Optimization of humanized IgGs in glycoengineered *Pichia pastoris*, *Nat. Biotechnol.*, 2006, **24**(2), 210–215.

- 27 M. Cerutti and J. Golay, Lepidopteran cells, an alternative for the production of recombinant antibodies?, *mAbs*, 2012, **4**(3), 294–309.
- 28 N. Yamane-Ohnuki and M. Satoh, Production of therapeutic antibodies with controlled fucosylation, *mAbs*, 2009, **1**(3), 230–236.
- 29 N. Yamane-Ohnuki, S. Kinoshita, M. Inoue-Urakubo, M. Kusunoki, S. Iida, R. Nakano, M. Wakitani, R. Niwa, M. Sakurada, K. Uchida, K. Shitara and M. Satoh, Establishment of FUT8 knockout Chinese hamster ovary cells: an ideal host cell line for producing completely defucosylated antibodies with enhanced antibody-dependent cellular cytotoxicity, *Biotechnol. Bioeng.*, 2004, **87**(5), 614–622.
- 30 P. Umana, J. Jean-Mairet, R. Moudry, H. Amstutz and J. E. Bailey, Engineered glycoforms of an antineuroblastoma IgG1 with optimized antibody-dependent cellular cytotoxic activity, *Nat. Biotechnol.*, 1999, **17**(2), 176–180.
- 31 D. Warnock, X. Bai, K. Autote, J. Gonzales, K. Kinealy, B. Yan, J. Qian, T. Stevenson, D. Zopf and R. J. Bayer, In vitro galactosylation of human IgG at 1 kg scale using recombinant galactosyltransferase, *Biotechnol. Bioeng.*, 2005, **92**(7), 831–842.
- 32 T. S. Raju, J. B. Briggs, S. M. Chamow, M. E. Winkler and A. J. Jones, Glycoengineering of therapeutic glycoproteins: in vitro galactosylation and sialylation of glycoproteins with terminal N-acetylglucosamine and galactose residues, *Biochemistry*, 2001, **40**(30), 8868–8876.
- 33 J. J. Goodfellow, K. Baruah, K. Yamamoto, C. Bonomelli, B. Krishna, D. J. Harvey, M. Crispin, C. N. Scanlan and B. G. Davis, An endoglycosidase with alternative glycan specificity allows broadened glycoprotein remodelling, *J. Am. Chem. Soc.*, 2012, **134**(19), 8030–8033.
- 34 C. W. Lin, M. H. Tsai, S. T. Li, T. I. Tsai, K. C. Chu, Y. C. Liu, M. Y. Lai, C. Y. Wu, Y. C. Tseng, S. S. Shivatare, C. H. Wang, P. Chao, S. Y. Wang, H. W. Shih, Y. F. Zeng, T. H. You, J. Y. Liao, Y. C. Tu, Y. S. Lin, H. Y. Chuang, C. L. Chen, C. S. Tsai, C. C. Huang, N. H. Lin, C. Ma, C. Y. Wu and C. H. Wong, A common glycan structure on immunoglobulin G for enhancement of effector functions, *Proc. Natl. Acad. Sci. U. S. A.*, 2015, **112**(34), 10611–10616.
- 35 I. Sassoian and V. Blanc, Antibody-drug conjugate (ADC) clinical pipeline: a review, *Methods Mol. Biol.*, 2013, **1045**, 1–27.
- 36 P. J. Carter and P. D. Senter, Antibody-drug conjugates for cancer therapy, *Cancer J.*, 2008, **14**(3), 154–169.
- 37 P. M. Drake and D. Rabuka, An emerging playbook for antibody-drug conjugates: lessons from the laboratory and clinic suggest a strategy for improving efficacy and safety, *Curr. Opin. Chem. Biol.*, 2015, **28**, 174–180.
- 38 N. Jain, S. W. Smith, S. Ghone and B. Tomczuk, Current ADC Linker Chemistry, *Pharm. Res.*, 2015, **32**(11), 3526–3540.
- 39 C. R. Behrens and B. Liu, Methods for site-specific drug conjugation to antibodies, *mAbs*, 2014, **6**(1), 46–53.
- 40 Q. Zhou and J. Kim, Advances in the Development of Site-Specific Antibody-Drug Conjugation, *Adv. Anticancer Agents Med. Chem.*, 2015, **15**(7), 828–836.
- 41 P. Akkapeddi, S. A. Azizi, A. M. Freedy, P. M. S. D. Cal, P. M. P. Gois and G. J. L. Bernardes, Construction of homogeneous antibody-drug conjugates using site-selective protein chemistry, *Chem. Sci.*, 2016, **7**(5), 2954–2963.
- 42 J. Y. Axup, K. M. Bajjuri, M. Ritland, B. M. Hutchins, C. H. Kim, S. A. Kazane, R. Halder, J. S. Forsyth, A. F. Santidrian, K. Stafin, Y. Lu, H. Tran, A. J. Seller, S. L. Biroc, A. Szydlak, J. K. Pinkstaff, F. Tian, S. C. Sinha, B. Felding-Habermann, V. V. Smider and P. G. Schultz, Synthesis of site-specific antibody-drug conjugates using unnatural amino acids, *Proc. Natl. Acad. Sci. U. S. A.*, 2012, **109**(40), 16101–16106.
- 43 F. Tian, Y. Lu, A. Manibusan, A. Sellers, H. Tran, Y. Sun, T. Phuong, R. Barnett, B. Hehli, F. Song, M. J. DeGuzman, S. Ensari, J. K. Pinkstaff, L. M. Sullivan, S. L. Biroc, H. Cho, P. G. Schultz, J. DiJoseph, M. Dougher, D. Ma, R. Dushin, M. Leal, L. Tchistiakova, E. Feyfant, H. P. Gerber and P. Sapra, A general approach to site-specific antibody drug conjugates, *Proc. Natl. Acad. Sci. U. S. A.*, 2014, **111**(5), 1766–1771.
- 44 E. S. Zimmerman, T. H. Heibeck, A. Gill, X. Li, C. J. Murray, M. R. Madlansacay, C. Tran, N. T. Uter, G. Yin, P. J. Rivers, A. Y. Yam, W. D. Wang, A. R. Steiner, S. U. Bajad, K. Penta, W. Yang, T. J. Hallam, C. D. Thanos and A. K. Sato, Production of site-specific antibody-drug conjugates using optimized non-natural amino acids in a cell-free expression system, *Bioconjugate Chem.*, 2014, **25**(2), 351–361.
- 45 D. Shinmi, E. Taguchi, J. Iwano, T. Yamaguchi, K. Masuda, J. Enokizono and Y. Shiraiishi, One-step conjugation method for site-specific antibody-drug conjugates through reactive cysteine-engineered antibodies, *Bioconjugate Chem.*, 2016, **27**(5), 1324–1331.
- 46 X. Li, T. Fang and G. J. Boons, Preparation of well-defined antibody-drug conjugates through glycan remodeling and strain-promoted azide–alkyne cycloadditions, *Angew. Chem., Int. Ed.*, 2014, **53**(28), 7179–7182.
- 47 Q. Zhou, J. E. Stefano, C. Manning, J. Kyazike, B. Chen, D. A. Gianolio, A. Park, M. Busch, J. Bird, X. Zheng, H. Simonds-Mannes, J. Kim, R. C. Gregory, R. J. Miller, W. H. Brondyk, P. K. Dhal and C. Q. Pan, Site-specific antibody-drug conjugation through glycoengineering, *Bioconjugate Chem.*, 2014, **25**(3), 510–520.
- 48 E. Boeggeman, B. Ramakrishnan, M. Pasek, M. Manzoni, A. Puri, K. H. Loomis, T. J. Waybright and P. K. Qasba, Site specific conjugation of fluoroprobes to the remodeled Fc N-glycans of monoclonal antibodies using mutant glycosyltransferases: application for cell surface antigen detection, *Bioconjugate Chem.*, 2009, **20**(6), 1228–1236.
- 49 Z. Zhu, B. Ramakrishnan, J. Li, Y. Wang, Y. Feng, P. Prabakaran, S. Colantonio, M. A. Dyba, P. K. Qasba and D. S. Dimitrov, Site-specific antibody-drug conjugation through an engineered glycotransferase and a chemically reactive sugar, *mAbs*, 2014, **6**(5), 1190–1200.

- 50 B. M. Zeglis, C. B. Davis, R. Aggeler, H. C. Kang, A. Chen, B. J. Agnew and J. S. Lewis, Enzyme-mediated methodology for the site-specific radiolabeling of antibodies based on catalyst-free click chemistry, *Bioconjugate Chem.*, 2013, **24**(6), 1057–1067.
- 51 R. van Geel, M. A. Wijdeven, R. Heesbeen, J. M. Verkade, A. A. Wasiel, S. S. Van Berkel and F. L. Van Delft, Chemoenzymatic Conjugation of Toxic Payloads to the Globally Conserved N-Glycan of Native mAbs Provides Homogeneous and Highly Efficacious Antibody-Drug Conjugates, *Bioconjugate Chem.*, 2015, **26**(11), 2233–2242.
- 52 P. Tumbale, H. Jamaluddin, N. Thiyagarajan, K. R. Acharya and K. Brew, Screening a limited structure-based library identifies UDP-GalNAc-specific mutants of alpha-1,3-galactosyltransferase, *Glycobiology*, 2008, **18**(12), 1036–1043.
- 53 A. Seko, M. Koketsu, M. Nishizono, Y. Enoki, H. R. Ibrahim, L. R. Juneja, M. Kim and T. Yamamoto, Occurrence of a sialylglycopeptide and free sialylglycans in hen's egg yolk, *Biochim. Biophys. Acta*, 1997, **1335**(1–2), 23–32.
- 54 B. Sun, W. Bao, X. Tian, M. Li, H. Liu, J. Dong and W. Huang, A simplified procedure for gram-scale production of sialylglycopeptide (SGP) from egg yolks and subsequent semi-synthesis of Man3GlcNAc oxazoline, *Carbohydr. Res.*, 2014, **396**, 62–69.
- 55 T. B. Parsons, W. B. Struwe, J. Gault, K. Yamamoto, T. A. Taylor, R. Raj, K. Wals, S. Mohammed, C. V. Robinson, J. L. Benesch and B. G. Davis, Optimal Synthetic Glycosylation of a Therapeutic Antibody, *Angew. Chem., Int. Ed.*, 2016, **55**(7), 2361–2367.
- 56 S. Puthenveetil, S. Musto, F. Loganzo, L. N. Tumej, C. J. O'Donnell and E. Graziani, Development of Solid-Phase Site-Specific Conjugation and Its Application toward Generation of Dual Labeled Antibody and Fab Drug Conjugates, *Bioconjugate Chem.*, 2016, **27**(4), 1030–1039.
- 57 X. L. Li, J. T. Patterson, M. Sarkar, L. Pedzisa, T. Kodadek, W. R. Roush and C. Rader, Site-Specific Dual Antibody Conjugation via Engineered Cysteine and Selenocysteine Residues, *Bioconjugate Chem.*, 2015, **26**(11), 2243–2248.
- 58 B. Li, Y. Zeng, S. Hauser, H. Song and L. X. Wang, Highly efficient endoglycosidase-catalyzed synthesis of glycopeptides using oligosaccharide oxazolines as donor substrates, *J. Am. Chem. Soc.*, 2005, **127**(27), 9692–9693.
- 59 H. Li, B. Li, H. Song, L. Breydo, I. V. Baskakov and L. X. Wang, Chemoenzymatic synthesis of HIV-1 V3 glycopeptides carrying two N-glycans and effects of glycosylation on the peptide domain, *J. Org. Chem.*, 2005, **70**(24), 9990–9996.
- 60 B. Li, H. Song, S. Hauser and L. X. Wang, A highly efficient chemoenzymatic approach toward glycoprotein synthesis, *Org. Lett.*, 2006, **8**(14), 3081–3084.
- 61 T. W. Rising, T. D. Claridge, N. Davies, D. P. Gamblin, J. W. Moir and A. J. Fairbanks, Synthesis of N-glycan oxazolines: donors for endohexosaminidase catalysed glycosylation, *Carbohydr. Res.*, 2006, **341**(10), 1574–1596.
- 62 W. Huang, H. Ochiai, X. Zhang and L. X. Wang, Introducing N-glycans into natural products through a chemoenzymatic approach, *Carbohydr. Res.*, 2008, **343**(17), 2903–2913.
- 63 H. Ochiai, W. Huang and L. X. Wang, Expedient chemoenzymatic synthesis of homogeneous N-glycoproteins carrying defined oligosaccharide ligands, *J. Am. Chem. Soc.*, 2008, **130**(41), 13790–13803.
- 64 T. W. Rising, C. D. Heidecke, J. W. Moir, Z. Ling and A. J. Fairbanks, Endohexosaminidase-catalysed glycosylation with oxazoline donors: fine tuning of catalytic efficiency and reversibility, *Chemistry*, 2008, **14**(21), 6444–6464.
- 65 M. Umekawa, W. Huang, B. Li, K. Fujita, H. Ashida, L. X. Wang and K. Yamamoto, Mutants of *Mucor hiemalis* endo-beta-N-acetylglucosaminidase show enhanced transglycosylation and glycosynthase-like activities, *J. Biol. Chem.*, 2008, **283**(8), 4469–4479.
- 66 W. Huang, C. Li, B. Li, M. Umekawa, K. Yamamoto, X. Zhang and L. X. Wang, Glycosynthases enable a highly efficient chemoenzymatic synthesis of N-glycoproteins carrying intact natural N-glycans, *J. Am. Chem. Soc.*, 2009, **131**(6), 2214–2223.
- 67 M. Noguchi, T. Tanaka, H. Gyakushi, A. Kobayashi and S. Shoda, Efficient Synthesis of Sugar Oxazolines from Unprotected N-Acetyl-2-amino Sugars by Using Chloroformamidinium Reagent in Water, *J. Org. Chem.*, 2009, **74**(5), 2210–2212.
- 68 K. Yamamoto, S. Kadowaki, M. Fujisaki, H. Kumagai and T. Tochikura, Novel Specificities of *Mucor Hiemalis* Endo-Beta-N-Acetylglucosaminidase Acting Complex Asparagine-Linked Oligosaccharides, *Biosci., Biotechnol., Biochem.*, 1994, **58**(1), 72–77.
- 69 W. Huang, Q. A. Yang, M. Umekawa, K. Yamamoto and L. X. Wang, *Arthrobacter* Endo-beta-N-Acetylglucosaminidase Shows Transglycosylation Activity on Complex-Type N-Glycan Oxazolines: One-Pot Conversion of Ribonuclease B to Sialylated Ribonuclease C, *ChemBioChem*, 2010, **11**(10), 1350–1355.
- 70 C. Besanceney-Webler, H. Jiang, T. Q. Zheng, L. Feng, D. S. Del Amo, W. Wang, L. M. Klivansky, F. L. Marlow, Y. Liu and P. Wu, Increasing the Efficacy of Bioorthogonal Click Reactions for Bioconjugation: A Comparative Study, *Angew. Chem., Int. Ed.*, 2011, **50**(35), 8051–8056.
- 71 N. J. Agard, J. A. Prescher and C. R. Bertozzi, A strain-promoted [3+2] azide-alkyne cycloaddition for covalent modification of biomolecules in living systems, *J. Am. Chem. Soc.*, 2004, **126**(46), 15046–15047.
- 72 J. M. Baskin, J. A. Prescher, S. T. Laughlin, N. J. Agard, P. V. Chang, I. A. Miller, A. Lo, J. A. Codelli and C. R. Bertozzi, Copper-free click chemistry for dynamic in vivo imaging, *Proc. Natl. Acad. Sci. U. S. A.*, 2007, **104**(43), 16793–16797.
- 73 X. H. Ning, J. Guo, M. A. Wolfert and G. J. Boons, Visualizing metabolically labeled glycoconjugates of living cells by copper-free and fast Huisgen cycloadditions, *Angew. Chem., Int. Ed.*, 2008, **47**(12), 2253–2255.